# Design of Smart Adaptive Control Systems

by

**Takuya KINOSHITA**

Graduate School of Engineering

Hiroshima University

March, 2017

# Acknowledgements

First, I would like to express my sincere gratitude to Professor Toru Yamamooto of Hiroshima University for his continuous support of my research, for his patience, motivation, and valuable suggestions. His guidance helped me through research and writing of this thesis. I would also like to acknowledge Professors Ichiro Nishizaki and Toshio Tsuji of Hiroshima University and Manabu Kano of Kyoto University, the members of my dissertation committee. Their stimulating suggestions have helped me in writing this thesis.

I express my gratitude to Professor Sirish L. Shah of University of Alberta who provided useful advice on the Smart-GMVIndex scheme. I also thank Associate Professor Yoshihiro Ohnishi of Ehime University for his useful advice on the PD-MVIndex scheme.

I appreciate the support of Associate Professor Shuichi Ohno and Assistant Professor Masayoshi Nakamoto of Hiroshima University. In addition, I express my sincere gratitude to all the past and present members of the control systems engineering laboratory. I would especially like to thank Mr. Guan Zhe, Mr. Liao Yuntao, and Mr. Rizwan Tariq, who are members of the Ph.D. course.

Finally, I am grateful to all the people who have supported me during my work on this thesis. Special thanks go to my family; their continuous support and encouragement made my studies possible.

# Contents

**Chapter**

**1** Introduction 1

1.1 Background . . . . . 1

1.2 Smart Adaptive Control Systems . . . . . 3

1.2.1 Direct controller design . . . . . 6

1.2.2 Integration of control assessment and control system design . . . . . 7

1.2.3 1-parameter tuning and controller redesign . . . . . 7

1.3 Dissertation Outline . . . . . 8

**2** Design of Smart Adaptive Control System based on Generalized Minimum Variance Control law 10

2.1 Introduction . . . . . 10

2.2 Design of a smart adaptive control system based on GMVC . . 12

2.2.1 System description . . . . . 12

2.2.2 Direct controller design based on GMVC . . . . . 12

2.2.3 Algorithm of smart adaptive control design . . . . . 18

2.3 Numerical example . . . . . 20

2.4 Conclusion . . . . . 24

**3** Design of Smart Adaptive Control system based on FRIT 27

3.1 Introduction . . . . . 27

3.2 Design of PD-MVIndex . . . . . 29

3.2.1 System description . . . . . 29

3.2.2 Control assessment index based on Minimum Variance control law: MV-Index . . . . . 30

3.2.3 Adjustment of PID parameters based on MV-Index using FRIT . . . . . 33

3.3 Design of smart-GMVIndex . . . . . 35

3.3.1 Overview of the Smart-GMVIndex control system . . . 35

3.3.2 Control assessment index based on Generalized Minimum Variance control law: GMV-Index . . . . . 36

3.3.3 Controller performance index based on GMVC . . . . . 38

3.3.4 Adjustment of PID parameters based on GMV-Index using FRIT . . . . . 38

3.3.5 Fictitious reference iterative control scheme . . . . . 38

3.3.6 1-parameter tuning based on GMV-Index . . . . . 40

3.4 Numerical example . . . . . 42

3.4.1 Application of PD-MVIndex controller . . . . . 42

3.4.2 Application of Smart-GMVIndex controller . . . . . 56

3.5 Conclusion . . . . . 61

**Appendix 3.A Deriving Eq. (3.11)** . . . . . 62

**Appendix 3.B Deriving Eq. (3.20)** . . . . . 63

**4** Application to a Temperature Control System 64

4.1 Introduction . . . . . 64

4.2 Application and consideration of smart adaptive controllers . . 66
4.2.1 Application of Smart-GMV controller . . . . . 66
4.2.2 Application of PD-MVIndex controller . . . . . 70
4.2.3 Comparing the proposed schemes . . . . . 72
4.3 Conclusion . . . . . 76

**5** Conclusions 78

**Bibliography** 82

**Publication Lists** **88**

**International Conference Papers** **90**

# Chapter 1

# Introduction

## 1.1 Background

Recently, it has become necessary to improve product quality and save energy in process industries, and control systems should be designed to achieve them strictly. In particular, system characteristics are changed significantly when the operating and/or environmental conditions are varied. A scheme is required to adjust the controller parameters online to achieve the user-specified control performance even when system characteristics are changed. To adapt with the system changes, an adaptive control system has been proposed. There are mainly two types of the adaptive control systems: model-reference adaptive control (MRAC) [1, 2, 3, 4, 5] and self-tuning control (STC) [6, 7, 8, 9, 10, 11]. In MRAC, the reference model is introduced and controller parameters are adjusted to minimize control output and reference model output. Hence, MRAC is often utilized in a deterministic framework without noise. In contrast, STC is usually used to minimize a cost function considering noise, and is designed in the probabilistic framework. In this thesis, STC is discussed because the controlled object is considered as a process systems

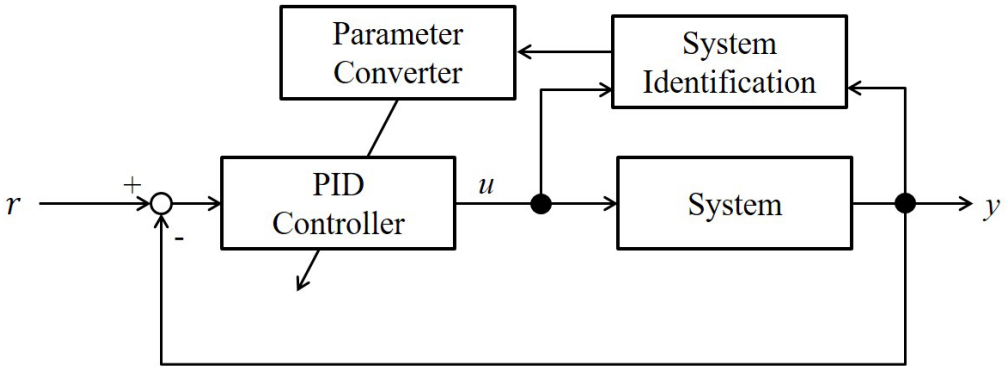


Figure 1.1: Block diagram of a self-tuning control system.

with noise.

Kalman proposed STC [6] in 1953, and K.J.Åström organized it [7]. Figure 1.1 shows the block diagram of a self-tuning control system. In a "system identification" module, system parameters are identified from the input/output (I/O) data of the system, and controller parameters are calculated using the system parameters from the "parameter converter" module. Therefore, control parameters are tuned adaptively even though system characteristics are changed. However, adjusting controller parameters recursively is not practical when the user-specified control performance is satisfied. Thus, it is important to adjust control parameters only when the control performance is deteriorated. In other words, an approach is required to integrate "control performance assessment" and "control system design".

Under above background, performance-driven control systems have been actively researched [12, 13, 14, 15, 16, 17, 18, 19]. In particular, Figure 1.2 shows a performance-driven control system [12] in which "control performance assessment" and "control system design" are combined. In this scheme, the control performance assessment is based on the error between control output

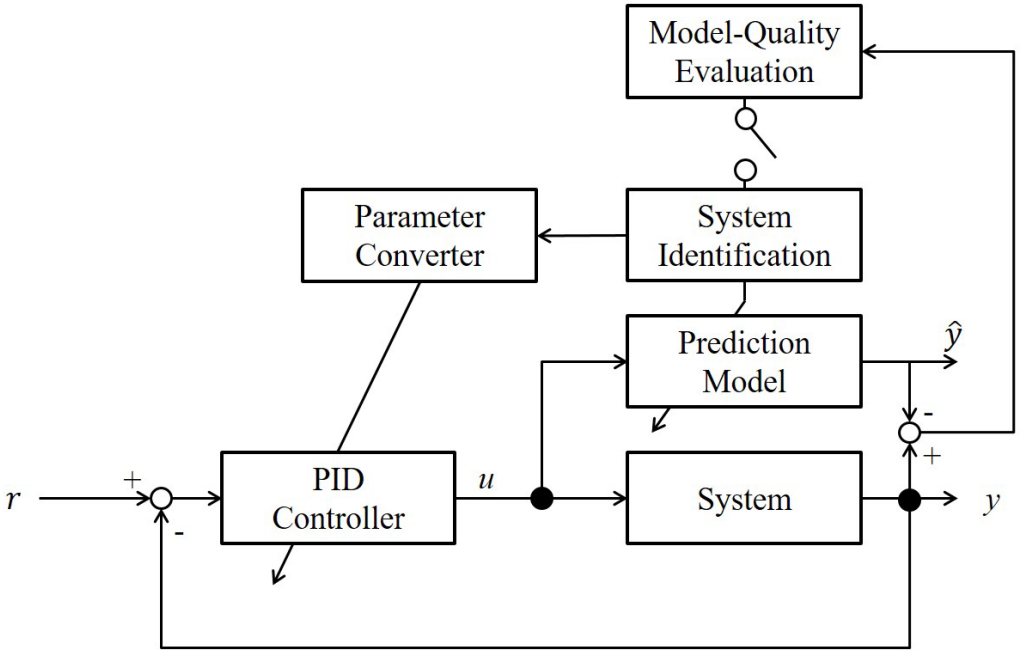


Figure 1.2: Block diagram of a performance-driven control system.

$y$ and prediction output $\hat{y}$ of the "prediction model". If the error is larger than a threshold set in advance, the control performance is judged as deteriorating in the "model-quality evaluation" module, and "prediction model" is re-calculated using the "system identification" module. At that time, the controller parameters are adjusted by the "parameter converter" module based on the system parameters. From the above mentioned algorithm shows that the performance-driven control is a more practical scheme than STC because of adjusting the controller parameters only when the prediction quality becomes undesirable.

## 1.2 Smart Adaptive Control Systems

In the previous section, it was stated that the performance-driven control is a more practical control scheme than the STC. However, it comprises

two limitations. The first is the control performance assessment. In process industries, the improvement of product quality and energy saving are influenced by control input and output strongly in the steady state. Therefore, control performance should be assessed using I/O data directly, and not by using system parameters. In the control performance assessment based on system parameters, the controller parameters are not adjusted if model quality is considered good even though control performance deteriorates. The second problem is the method of calculating controller parameters. In the conventional performance-driven controller, the calculation of controller parameters is the same as in STC, and it is based on system parameters. Hence, the controller quality is related to the accuracy of system identification. Generally, to improve the system identification accuracy, the control input should satisfy a persistently exciting (PE) [20, 21] condition. However, it is difficult to input such a high frequency signal to the actual controlled object. Thus, in this thesis, a method is proposed to calculate the controller parameters without system identification to solve these two problems.

The proposed scheme is based on the performance-driven controller, and the controller parameters are retuned only when control performances deteriorates. Figure 1.3 shows the block diagram of the proposed scheme. In the controller performance assessment of the proposed scheme, the variance of control input and output is considered for the process system, which is in steady state. Furthermore, to maintain the user-specified control performance, adjustable parameters included in the controller are adjusted (1-parameter tuning) when the deterioration of control performance is small. However, when the dete-

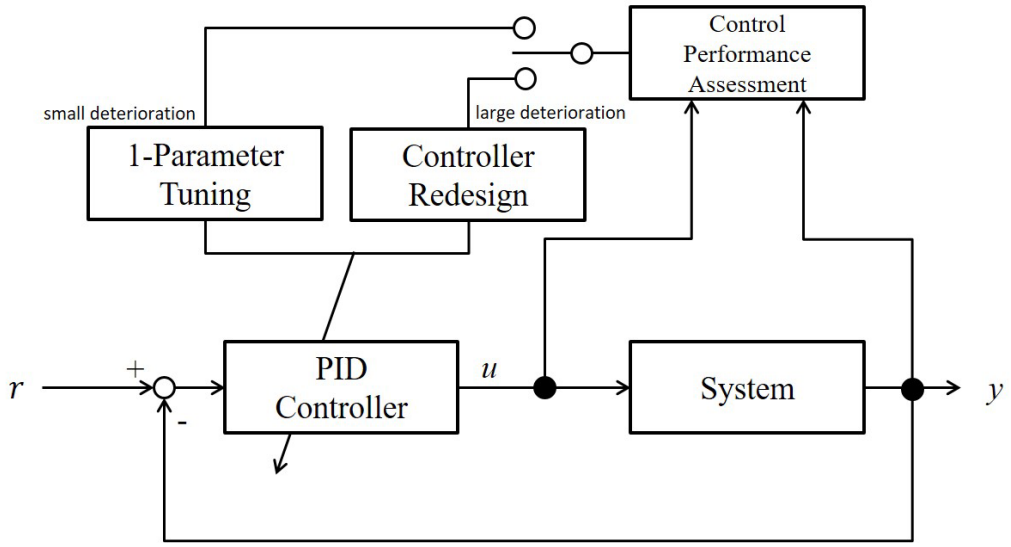


Figure 1.3: Block diagram of a smart adaptive control system.

rioration of control performance is significant, all controller parameters are recalculated (controller redesign) using closed-loop data directly. Thus, the features of the proposed scheme are summarized as follows:

(1) The controller parameters are directly calculated using closed-loop data.

(2) "Control performance assessment" and "control system design" are integrated.

(3) "1-parameter tuning" and "controller redesign" are switched appropriately, depending on the deterioration of control performance.

Therefore, the proposed scheme is called as the "smart adaptive control" in this thesis. The three aforementioned features are described in detail in the following subsections.

### 1.2.1 Direct controller design

In the model-based control scheme, high accuracy of system identification is required to obtain good control performance. Thus, a random signal such as a M-sequence signal should be input from the view-point of PE condition. However, the generation of the product is stopped because of the M-sequence input signal for system identification, which is time and cost consuming. Hence, the data-oriented control scheme were recently proposed in which controller parameters are determined without system identification. In the iterative feedback tuning (IFT) [22, 23, 24, 25, 26], suitable controller parameters are calculated recursively so that a criterion is minimized. However, conducting several experiments for calculation of controller parameters in IFT will take considerable amounts of time. On the other hand, in the virtual reference feedback tuning (VRFT) [27, 28, 29, 30, 31], controller parameters are obtained using the virtual reference signal based on a set of experimental data. However, in VRFT, a desired initial experimental data should be open-loop data, and it is difficult to obtain the data in real process systems. Therefore, the fictitious reference iterative tuning (FRIT) [32, 33, 34] was proposed in which the controller parameters are calculated using closed-loop data. Moreover, a direct controller design based on the generalized minimum variance control law (GMVC) has been proposed [35]. These direct controller design schemes have attracted attention and have been considerably researched [36, 37, 38, 39, 40, 41, 42].

### 1.2.2 Integration of control assessment and control system design

Presently, a better control performance is required to produce high quality production. Thus, it is necessary to assess the control performance, for which some schemes have been proposed. In particular, the minimum variance control index (MV-Index) [43, 44, 45] and GMVC Index (GMV-Index) are based on the variance control input and output in the steady state; this is easily understandable as their indexes are normalized. For example, the best and worst control performances are evaluated as 1 and 0, respectively. However, these assessments did not specify how to adjust the controller parameters for system changes due to off-line evaluation. Therefore, Shah *et al.* [13] proposed the performance-driven control scheme in which "control performance assessment" and "controller redesign" are integrated. In the performance-driven control scheme, an adjustable parameter included in the controller is determined using the trade-off curve which represents the relationship between the variance of input and control error in the steady state. In the next subsection, "1-parameter tuning" and "controller redesign" are introduced using the trade-off curve.

### 1.2.3 1-parameter tuning and controller redesign

In this thesis, "1-parameter tuning" and "controller redesign" are applied to the control systems appropriately, depending on the deterioration of control performance. The conventional scheme was proposed by Yamamoto [12], in which an adjustable parameter is included in GMVC. Generally, it is

difficult for operators to judge which controller parameters should be tuned if there are many controller parameters, or only skilled operators can adjust them. Hence, it is easy to tune an adjustable controller parameter in GMVC because it has a physical meaning. Furthermore, in the steady state, the I/O data does not include much of the time-delay and time constant information. Thus, the reliability of the controller is low if all controller parameters are calculated using the I/O data of steady state. Therefore, 1-parameter tuning is an effective tuning method in the steady state because it does not recalculate all controller parameters.

## 1.3 Dissertation Outline

The current thesis is composed of the following five chapters.

In Chapter 2, a smart adaptive control scheme based on the GMVC law is proposed. First, a scheme is explained in which controller parameters are calculated directly without system identification. Next, "1-parameter tuning' and "controller redesign" are switched by according to the trade-off curve, which shows the relationship between variance of control error and input. Hence, the derivation of the trade-off curve and the algorithm to achieve the desired control performance by using a smart adaptive control law based on GMVC are described. The effectiveness of this scheme is verified by satisfying the desired control performance for a time-variant system in a numerical example.

Chapter 3 describes a smart adaptive control scheme based on FRIT. An archival desired control performance (variance of control error and input)

is different in each controlled objects, and it is difficult to set the threshold for switching "1-parameter tuning" and "all controller parameters design". Therefore, in Chapter 3, the control performance assessment (MV-Index and GMV-Index) is focused upon and the controller parameters are calculated such that the control performance assessment is improved using FRIT. The effectiveness of this scheme is confirmed using a numerical example.

Chapter 4 discusses the application of each smart adaptive control scheme in Chapters 2 and 3 to the temperature control system. In the temperature control system, control output and input are the water temperature and open/close ratio of hot water valve, respectively. Moreover, a system characteristic is changed by increasing/decreasing the flow rate of cold water. Finally, the control results of each smart adaptive control scheme are compared.

Chapter 5 concludes this thesis, and mentions some of the outstanding issues.

# Chapter 2

# Design of Smart Adaptive Control System based on Generalized Minimum Variance Control law

## 2.1 Introduction

The proportional-integral-derivative (PID) controller [46, 47, 48, 49] has been utilized widely in process industries as the physical meaning of PID parameters is clear and the control structure is simple. For example, proportional, integral, and derivative feedback are based on the present, past, and future, respectively. Thus, more than 80% of all controllers in process industries are PID controllers [50]. However, it is difficult to maintain the desired control performance by using fixed PID parameters for time-variant systems. Therefore, control parameters must be adjusted online such as the self-tuning control [6, 7, 8, 9, 10, 11]. In those scheme, control parameters are adjusted in every step even though the control performance is good. Thus, it is better to adjust control parameters only when control performance becomes unsatisfactory. Consequently, the idea of "Tuning on Demand" is contemplated, according to which control parameters are adjusted only when control per-

formance is insufficient. In other words, performance-adaptive control [12], which integrates "control performance assessment" and "control system design", becomes more necessary.

There are two methods for calculating control parameters. One is based on a system model, and the other is based on closed-loop data without system identification [23, 27, 51, 52].

In this chapter, two aspects are considered: control performance assessment using closed-loop data and the method of adjusting control parameters. In particular, control performance is improved through 1-parameter tuning based on the GMVC without system identification [52]. 1-parameter tuning is a simple technique of maintaining control performance. The features of the proposed method are as follows:

(1) "Evaluate control performance" and "Design control system" are based only on closed-loop data.

(2) Adjust control parameters effectively by 1-parameter tuning.

This proposed control system is called a smart adaptive control system based on GMVC (Smart-GMV) because control performance assessment and adjustment of control parameters work automatically.

## 2.2 Design of a smart adaptive control system based on GMVC

### 2.2.1 System description

The controlled object is described by the following equation:

$$A(z^{-1})y(t) = z^{-1}B(z^{-1})u(t) + \xi(t)/\Delta \tag{2.1}$$

$$\left.\begin{aligned} A(z^{-1}) &= 1 + a_1 z^{-1} + a_2 z^{-2} \\ B(z^{-1}) &= b_0 + b_1 z^{-1} + \cdots + b_m z^{-m} \end{aligned}\right\}. \tag{2.2}$$

In Eq. (2.1), $u(t)$ is the control input, $y(t)$ is the system output, $\xi$(t) shows Gaussian white noise, with zero mean and covariance $\sigma^2$. In addition, $z^{-1}$ is the back shift operator, which implies $z^{-1}y(t)$=$y(t-1)$. $\Delta$ denotes a difference operator and $\Delta$:= $1 - z^{-1}$ is defined. Additionaly, $m$ expresses the order of $B(z^{-1})$. Note that the order of $A(z^{-1})$ is two in this section because PID controller is designed next subsection.

### 2.2.2 Direct controller design based on GMVC

In the system of Eq. (2.1), the GMVC law is derived based on the minimization of the following criterion:

$$J = \mathcal{E}\left[\phi^2(t+1)\right], \tag{2.3}$$

where $\mathcal{E}[\cdot]$ denotes the expectation. $\phi(t+1)$ is a generalized output given by the following equation:

$$\phi(t+1) := P(z^{-1})y(t+1) + \lambda\Delta u(t) - P(1)r(t), \tag{2.4}$$

where $r(t)$ denotes the reference signal of the step. In addition, $\lambda$ is the weighting factor for input variation and it is user-specified parameter. Eq.

(2.4) can be rewritten by using the reference signal $y_m(t)$ as follows:

$$\begin{aligned}\phi(t+1) &= P(z^{-1})\left\{y(t+1)+\frac{\lambda}{P(z^{-1})}\Delta u(t)-\frac{P(1)}{P(z^{-1})}r(t)\right\}\\ &= P(z^{-1})\left\{y(t+1)+\frac{\lambda}{P(z^{-1})}\Delta u(t)-y_m(t)\right\} \qquad (2.5)\\ y_m(t) &:= \frac{P(1)}{P(z^{-1})}r(t). \qquad (2.6)\end{aligned}$$

In addition, $P(z^{-1})$ is a polynomial and is designed based on the reference design [11] as follows:

$$P(z^{-1}) = 1 + p_1 z^{-1} + p_2 z^{-1} \qquad (2.7)$$

$$\left.\begin{aligned} p_1 &= -2e^{-\frac{\rho}{2\mu}}\cos\left(\tfrac{\sqrt{4\mu-1}}{2\mu}\rho\right)\\ p_2 &= e^{-\frac{\rho}{\mu}}\\ \rho &:= T_s/\sigma\\ \mu &:= 0.25(1-\delta)+0.51\delta \end{aligned}\right\}, \qquad (2.8)$$

where $\sigma$ is a parameter related to the rise-time and $\delta$ is a parameter related to the damping oscillation. The operators set them arbitrarily. $\sigma$ denotes the time when output reaches approximately 60% of the step reference value. Furthermore, $\delta$ is desirably set between $0 \leq \delta \leq 2.0$. In particular, $\delta = 0$ indicates the response of Butterworth model and $\delta = 1.0$ indicates the response of Binominal model.

The Diophantine Eq. (2.9) is introduced by the formula:

$$P(z^{-1}) = \Delta A(z^{-1}) + z^{-1}F(z^{-1}), \qquad (2.9)$$

where

$$F(z^{-1}) = f_0 + f_1 z^{-1} + f_2 z^{-2}. \qquad (2.10)$$

From Eqs. (2.1), (2.4), and (2.9), the one-step ahead prediction of the generalized output at time $t$ is expressed by the following equation:

$$\phi(t+1|t) = F(z^{-1})y(t) + \left\{B(z^{-1}) + \lambda\right\}\Delta u(t) \\ -P(1)r(t) + \xi(t+1). \tag{2.11}$$

Here, the optimal one-step ahead prediction value at time $t$ is defined as follows:

$$\hat{\phi}(t+1|t) := F(z^{-1})y(t) + \left\{B(z^{-1}) + \lambda\right\}\Delta u(t) \\ -P(1)r(t). \tag{2.12}$$

In addition, the following equation is obtained from Eqs. (2.11) and (2.12).

$$\phi(t+1|t) = \hat{\phi}(t+1|t) + \xi(t+1). \tag{2.13}$$

From Eqs. (2.3) and (2.13), the GMVC law (2.14) is derived as a criterion $J$, which is minimized by the $\hat{\phi}(t+1|t) = 0$.

$$\Delta u(t) = \frac{P(1)}{B(z^{-1}) + \lambda}w(t) - \frac{F(z^{-1})}{B(z^{-1}) + \lambda}y(t). \tag{2.14}$$

In this chapter, the control parameters are calculated directly based on a implicit method of GMVC without the system identification. First, prediction error between the generalized output and the optimal predicted value is defined as follows:

$$\varepsilon(t+1) := \phi(t+1) - \hat{\phi}(t+1|t). \tag{2.15}$$

The parameters $F(z^{-1})$ and $B(z^{-1})$ are calculated directly from the closed-loop data by applying the least square method to the minimum of $\frac{1}{2}\varepsilon(t+1)^2$

[9]. It is possible to design the GMVC system directly based on closed-loop data by applying $F(z^{-1})$ and $B(z^{-1})$ to Eq. (2.14).

Next, the PID parameters are replaced by the implicit GMVC [11, 12, 52]. First, consider the following velocity type PID control law:

$$\Delta u(t) = \frac{k_c T_s}{T_I} e(t) - k_c \left( \Delta + \frac{T_D}{T_s} \Delta^2 \right), \tag{2.16}$$

where

$$e(t) := r(t) - y(t). \tag{2.17}$$

Variables $k_c$, $T_I$, and $T_D$ respectively denote the proportional gain, integral time, and derivative time. Next, the following equation, obtained by replacing the steady-state term $B(1)$ with the polynomial $B(z^{-1})$ in Eq. (2.14).

$$\Delta u(t) = \frac{P(1)}{B(1) + \lambda} w(t) - \frac{F(z^{-1})}{B(1) + \lambda} y(t). \tag{2.18}$$

By comparing the coefficients of Eqs. (2.16) and (2.18), the PID parameters can approximately be replaced by GMVC parameters as follows:

$$\left.\begin{aligned} k_c &= -\frac{f_1 + 2f_2}{B(1) + \lambda} \\ T_I &= -\frac{f_1 + 2f_2}{f_0 + f_1 + f_2} T_s \\ T_D &= -\frac{f_2}{f_1 + 2f_2} T_s \end{aligned}\right\}. \tag{2.19}$$

In this chapter, $\lambda$ is adjusted based on "variance of the control error" and "variance of the control input". The trade-off curve shown in Figure 2.1 is obtained by changing $\lambda$. In this figure, the vertical axis shows the variance of control error in the steady-state $\mathcal{E}[e^2(t)]$ and the horizontal axis shows the variance of the control input variation $\mathcal{E}[(\Delta u(t))^2]$. Figure 2.1 shows that it

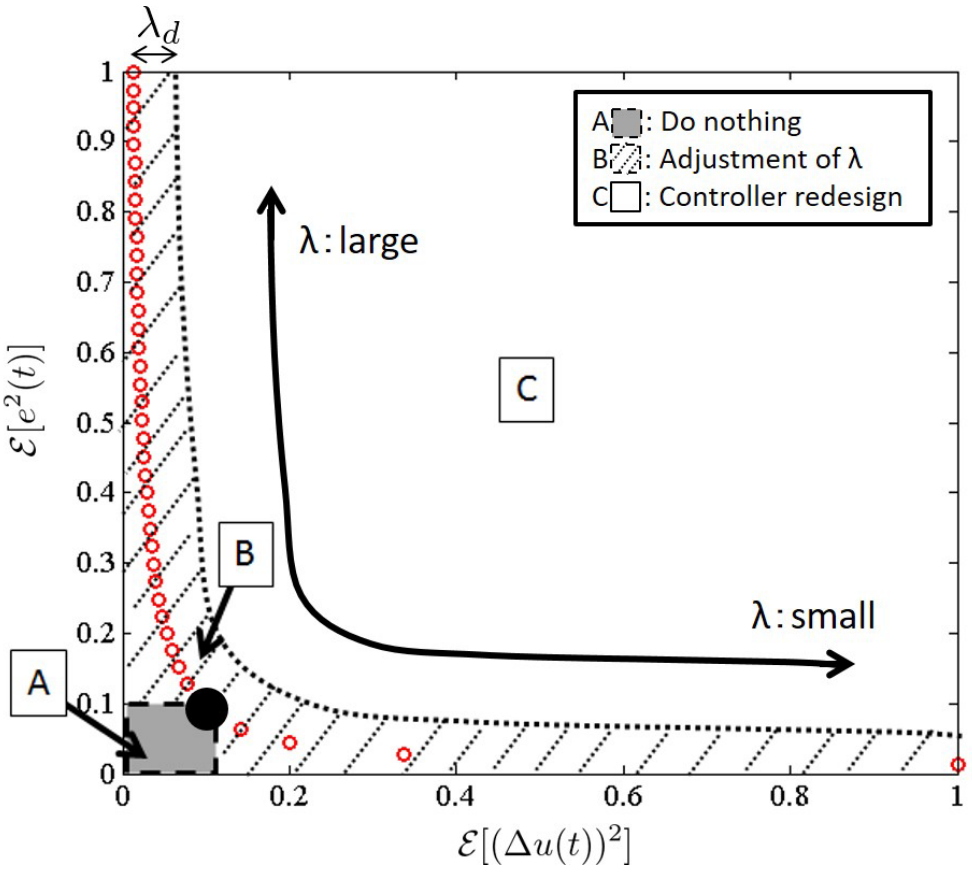


Figure 2.1: Trade-off curve indicated by changing $\lambda$.

is simple to adjust control performance by $\lambda$. The "A", "B" and "C" regions are described later.

In Figure 2.1, $\mathcal{E}[e^2(t)]$ and $\mathcal{E}[(\Delta u(t))^2]$ are adjusted based on $\lambda$, which can be determined by the trade-off curve. First, the user specifies the desired variance of control error: $\sigma_e^2$. Then, $\lambda$ is determined from $\sigma_e^2$. In Figure 2.1, the point "•" is a desired control performance ($\sigma_e^2 = 0.1$). Consequently, if current control performance can be plotted within region A, the desired control performance is satisfied.

However, it can be considered that the desired control performance

is not satisfied due to the time-variant system. This implies that current control performance is moved to region B or C from region A in Figure 2.1. Therefore, this chapter presents the method that maintains the desired control performance when current control performance is plotted in (i) region B and (ii) region C.

(i) If current control performance is in region B, control parameters are adjusted through the 1-parameter tuning, which adjusts $\lambda$.

(ii) If current control performance is in region C, it is difficult to achieve the desired control performance through the 1-parameter tuning. Therefore, control parameters are recalculated directly from closed-loop data in Eq. (2.19).

In addition, $\lambda_d$ is the width between trade-off curve and the boundary line of regions B and C, as shown in Figure 2.1.

To obtain the trade-off curve, the variance of control error $e(t)$ and the variance of input variation $\Delta u(t)$ can be calculated by the following equation using $H_2$ norm $||\cdot||_2$ [12]:

$$\mathcal{E}[e^2(t)] = \left|\left|-\frac{1}{T(z^{-1})}\right|\right|_2^2 \sigma_\xi^2 \tag{2.20}$$

$$\mathcal{E}[(\Delta u(t))^2] = \left|\left|-\frac{C(z^{-1})}{T(z^{-1})}\right|\right|_2^2 \sigma_\xi^2, \tag{2.21}$$

where

$$T(z^{-1}) := \Delta A(z^{-1}) + z^{-1}B(z^{-1})C(z^{-1}) \tag{2.22}$$

$$C(z^{-1}) := \frac{F(z^{-1})}{B(1)+\lambda}. \tag{2.23}$$

In Eq. (2.22), system parameter $A(z^{-1})$ is required for calculating $T(z^{-1})$. Therefore, the Eq. (2.22) can be rewritten as follows:

$$T(z^{-1}) = P(z^{-1}) + z^{-1}\left\{B(z^{-1})C(z^{-1}) - F(z^{-1})\right\}, \tag{2.24}$$

where $F(z^{-1})$ and $B(z^{-1})$ are calculated by the minimization of $\frac{1}{2}\varepsilon(t+1)^2$ in Eq. (2.15). Thus, the trade-off curve is obtained without system parameter $A(z^{-1})$ from Eqs. (2.23) and (2.24). In addition, $\sigma_\xi$ denotes the covariance of Gaussian white noise. However, the value of $\sigma_\xi$ is unknown. Therefore, $\sigma_\varepsilon$, which is the standard deviation of $\varepsilon$ in Eq. (2.15), is utilized instead of $\sigma_\xi$.

### 2.2.3 Algorithm of smart adaptive control design

The algorithm is represented using Figure 2.1. In the proposed algorithm, $N$ is the number of data. Moreover, each variance is calculated as the time average assuming that ergodicity holds.

$1^o$ Obtain the closed-loop data by initial controller.

$2^o$ Calculate $F(z^{-1})$ and $B(z^{-1})$ from the closed-loop data based on GMVC.

$3^o$ Calculate $\sigma_\varepsilon$, which is the standard deviation in Eq. (2.15).

$4^o$ Calculate Eqs. (2.20) and (2.21) to obtain the trade-off curve, as shown in Figure 2.1.

$5^o$ Calculate the point $(\mathcal{E}[(\Delta u(t))^2]_{\min}, \mathcal{E}[e^2(t)]_{\min})$, that is, "•" in Figure 2.1, from the desired control error variance $\sigma_e^2$ set in advance. Adopt

$\lambda$ calculated from the trade-off curve for the PID parameters in Eq. (2.19).

$6^o$ The following criterion $J_r$ is obtained using $\mathcal{E}[(\Delta u(t))^2]_{\min}$ and $\mathcal{E}[e^2(t)]_{\min}$ as the slope of the straight line passing through the origin and "•" in Figure 2.1.

$$J_r = \frac{\mathcal{E}[e^2(t)]_{\min}}{\mathcal{E}[(\Delta u(t))^2]_{\min}} \tag{2.25}$$

$7^o$ During $N$ steps, control by using the PID controller employed in $5^o$.

$8^o$ Calculate the current variance of control error $\mathcal{E}[e^2(t)]$ and variance of control input variation $\mathcal{E}[(\Delta u(t))^2]$ by using $N$ data from time: $t$ before the $N$ steps.

Next, calculate the following current criterion $J(t)$ by using $\mathcal{E}[(\Delta u(t))^2]$ and $\mathcal{E}[e^2(t)]$, the same as in $6^o$.

$$J(t) = \frac{\mathcal{E}[e^2(t)]}{\mathcal{E}[(\Delta u(t))^2]} \tag{2.26}$$

$9^o$ If the current variance $\mathcal{E}[(\Delta u(t))^2]$ and $\mathcal{E}[e^2(t)]$ of $8^o$ are located in region A, B or C, go to $11^o$, $10^o$, or $2^o$, respectively (Use $N$ data when going to $2^o$).

$10^o$ Adjust $\lambda$, and calculate PID gains corresponding to $\lambda$. Here, $\lambda$ is increased/decreased by $\Delta\lambda$ to close current performance to "•". In particular, if the following equation is satisfied, $\lambda = \lambda + \Delta\lambda$. Otherwise, $\lambda = \lambda - \Delta\lambda$.

$$J(t) < J_r \tag{2.27}$$

$11^o$ $t = t + 1$

$12^o$ Return to $8^o$.

### 2.3 Numerical example

In this section, the proposed Smart-GMV control scheme is applied to initial setting of PID parameters. In addition, $r(t) = 10$, $m = 3$, $N = 500$, $\lambda_d = 0.03$, and $\Delta\lambda = 0.02$ are set. First, consider the following system:

$$G(s) = \frac{K}{1 + Ts} e^{-Ls}, \tag{2.28}$$

where $T = 100$[s], $K = 0.9$, and $L = 15$[s]. Discretize Eq. (2.28) by sampling time $T_s = 5.0[s]$ and $\xi(t)$ in Eq. (2.1) is the Gaussian white noise with mean 0 and covariance 0.001. Furthermore, the system gain and time constant are changed between 2001[step] to 5000[step] as follows:

$$T = \begin{cases} 100 & (0 < t \leq 2000) \\ 100 - \dfrac{50(t - 2000)}{3000} & (2001 < t \leq 5000) \\ 50 & (5000 < t \leq 8000) \end{cases} \tag{2.29}$$

$$K = \begin{cases} 0.9 & (0 < t \leq 2000) \\ 0.9 + \dfrac{5.1(t - 2000)}{3000} & (2001 < t \leq 5000) \\ 6 & (5000 < t \leq 8000) \end{cases} . \tag{2.30}$$

The proposed Smart-GMV control scheme is applied for the controlled object. The control results are shown in Figure 2.2. In addition, $\sigma_e^2 = 0.4$ is set as the desired variance of control error. In the first 1000 steps, the initial PID parameters were set as following equation to obtain closed-loop data:

$$k_c = 8.89, T_I = 30.0, T_D = 7.50. \tag{2.31}$$

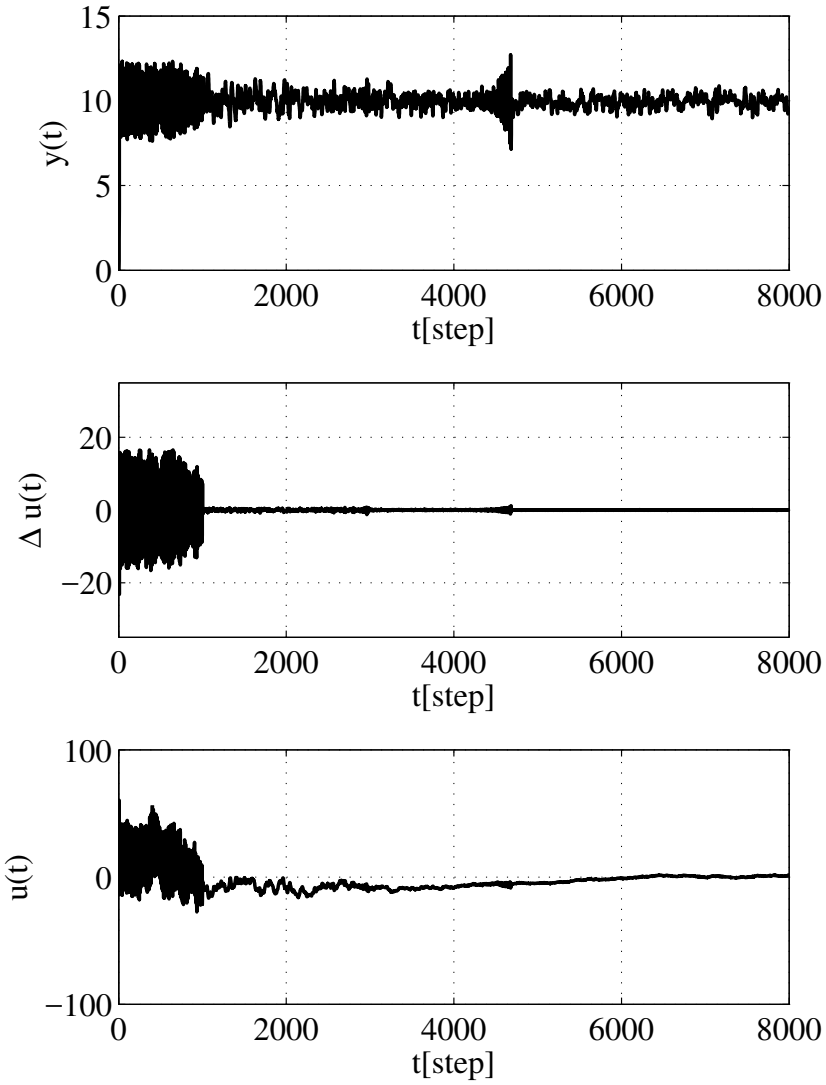


Figure 2.2: Control result by the proposed Smart-GMV control scheme when $\sigma_e^2 = 0.4$.

which is calculated by the Ziegler-Nichols (ZN) method [46].

Next, the proposed control is performed at $t = 1000$[step]. In addition,

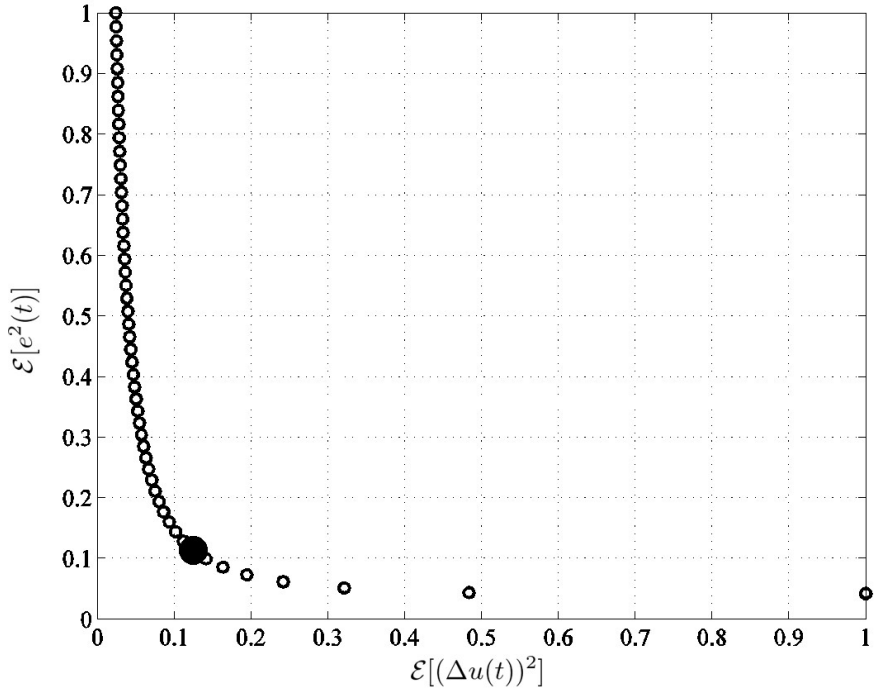


Figure 2.3: Trade-off curve indicated by changing $\lambda$.

$P(z^{-1})$ is designed as follows:

$$P(z^{-1}) = 1 - 1.64z^{-1} + 0.67z^{-2}. \tag{2.32}$$

In this case, the trade-off curve shown in Figure 2.3 is obtained from the closed-loop data. "•" denotes the desired control performance. After 1000[step], the variance of control error is 0.22, and the desired control performance ($\sigma_e^2 = 0.4$) is achieved. Figures 2.4 and 2.5 show the trajectories of PID parameters and $\lambda$, respectively. Figure 2.6 shows the trajectories of variance of control error and input.

In Figure 2.4, $T_I$ and $T_D$ were adjusted at 4683[step]; however, $k_c$ was adjusted several times before 4683[step]. This is because $\lambda$ is adjusted in $10^o$ and only $k_c$ depends on $\lambda$ in Eq. (2.19). In contrast, the variance of control

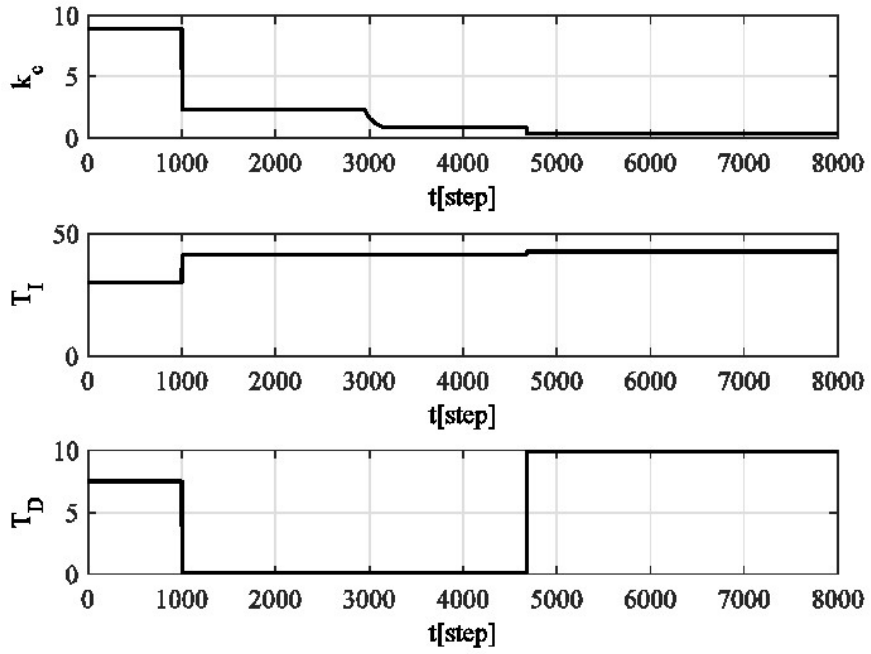


Figure 2.4: Trajectories of PID parameters corresponding to Figure 2.2.

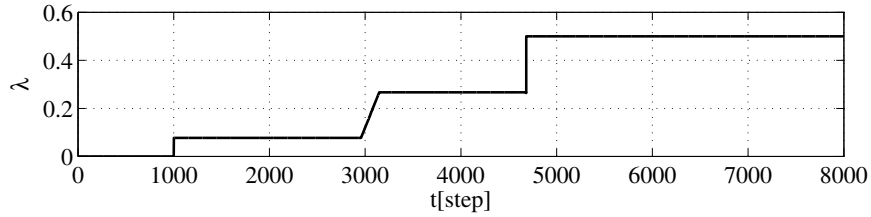


Figure 2.5: Trajectories of the user-specified parameter $\lambda$ corresponding to Figure 2.2.

input variation $\mathcal{E}[\Delta u(t)^2]$ exceeds the desired $\mathcal{E}[\Delta u(t)^2]_{\min}$ at approximately 3000[step], while $\mathcal{E}[e(t)^2]$ does not exceed the desired $\mathcal{E}[e(t)^2]_{\min}$ in Figure 2.6. "1-parameter tuning" was worked first at approximately 3000[step] because the current control performance located in region B in $9^o$. Moreover, at 4683[step], both $\mathcal{E}[e(t)^2]$ and $\mathcal{E}[\Delta u(t)^2]$ exceed the desired $\mathcal{E}[e(t)^2]_{\min}$ and

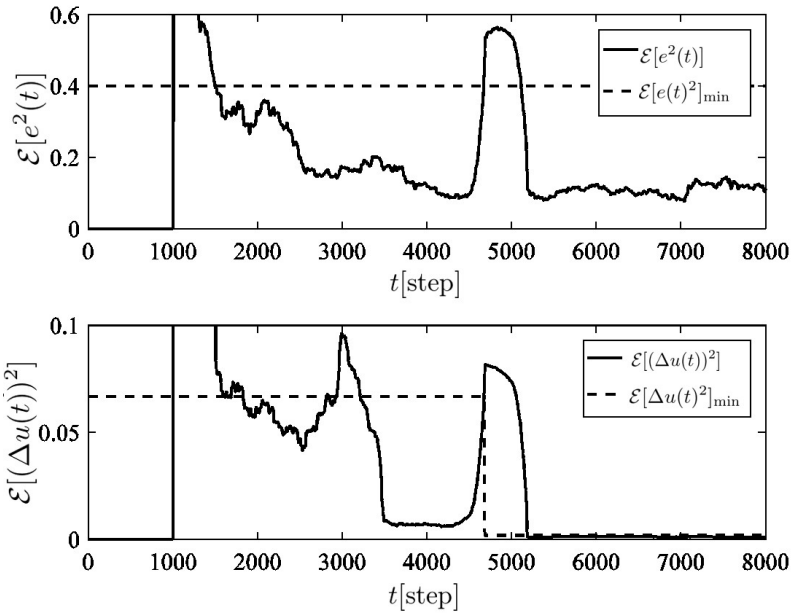


Figure 2.6: Trajectories of variance of $e(t)$ and $\Delta u(t)$ corresponding to Figure 2.2.

$\mathcal{E}[\Delta u(t)^2]_{\min}$, respectively. The "control parameters redesign" functioned at 4683[step] because the current control performance located in region C in $9^o$. As a result, PID parameters could be adjusted efficiently for the time-variant system.

Finally, Figure 2.7 shows the control result obtained using only the ZN method [46] for the purpose of comparison. It is impossible to control the time-variant system by using the fixed PID parameters. The aforementioned results verify the effectiveness of the proposed method.

## 2.4 Conclusion

This chapter proposed a Smart-GMV control system for a time-variant system. In the numerical example, user-specified variance of control error

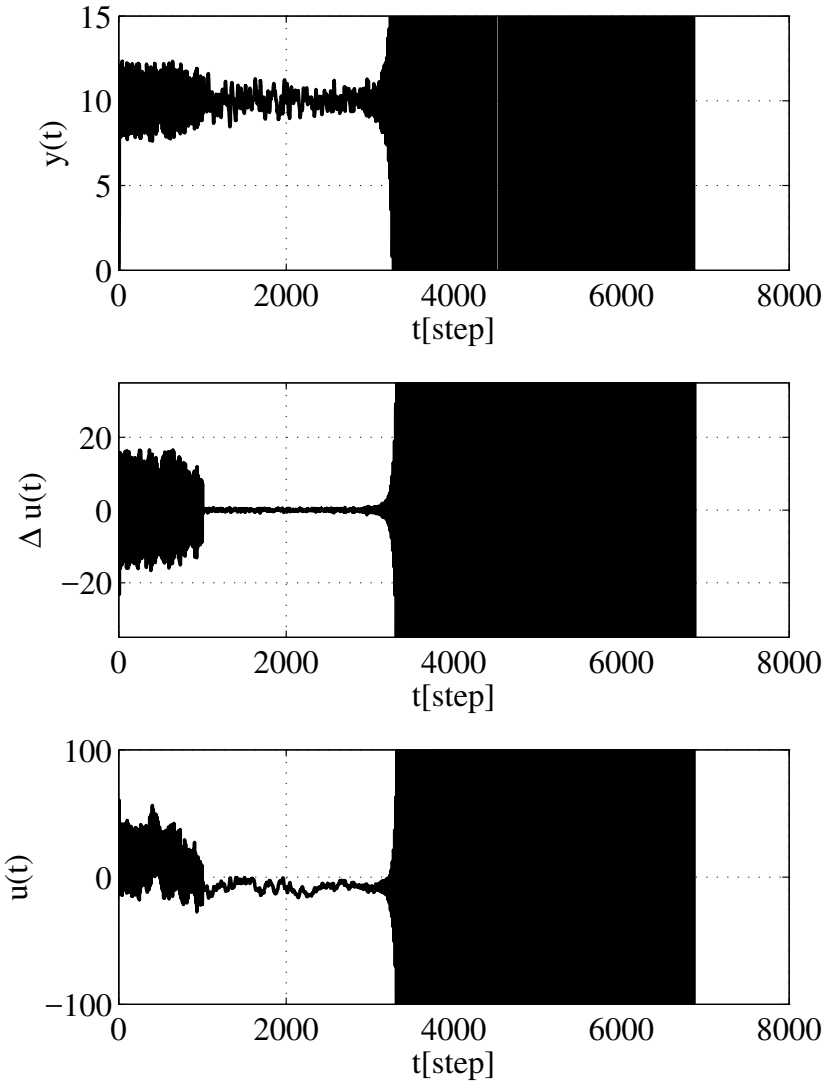


Figure 2.7: Control result obtained using the fixed PID parameters tuned by the ZN method.

is achieved as the desired control performance, while system parameters are changed. The features of the proposed Smart-GMV control scheme are as follows:

(1) "Evaluate control performance" and "design control system" are based on only closed-loop data.

(2) A user-specified parameter $\lambda$ is automatically adjusted without system identification.

In the proposed Smart-GMV control scheme, it is difficult to set $\Delta\lambda$, which is an adjusted value of $\lambda$. Therefore, in the future, a method for adjusting $\lambda$ without $\Delta\lambda$ will be considered.

# Chapter 3

# Design of Smart Adaptive Control system based on FRIT

## 3.1 Introduction

In the process industry, it is important to track the system output to the reference signal and maintain the desired control performance in steady state because this results in the production of a high-quality product and energy saving. In reality, the variance of system output is increased because of the noise, disturbance, order of controller, and the value of controller parameters. The designing an appropriate control system that reduces the variance is important for achieving the desired control performance [53]. Some studies [43, 54, 55, 56] have proposed control performance assessment by using the variance. Moreover, a practical application based on the above mentioned control performance assessment has been discussed [57]. In particular, the control performance assessment based on the minimum variance control law (MV-Index) [43] is characterized by its assessment simplicity and lack of the need of a system model for calculating an assessment index.

Meanwhile, the controlled system characteristic is not always time-

invariant. Furthermore, the control performance is deteriorated depending on the various of operation conditions and surrounding circumstances. This deterioration is coped with by using an online method for adjusting a control parameter (i.e., self-tuning control[7, 8, 9, 10, 58, 59], adaptive control[3, 5, 60, 61, 62], and performance-driven control[12, 63]). The performance-driven control is particularly characterized by the adjustment of the control parameters only when control performance is deteriorated. However, in the proposed Smart-GMV control scheme, described in chapter 2, it is difficult to set the threshold of variance $\lambda_d$ in advance because the variance is not a normalized control assessment. In addition, it is easer to set the threshold in the MV-Index comparing $\lambda_d$ because of normalized assessment, which defines that the best and worst control performances are evaluated as 1 and 0, respectively. Nevertheless, the MV-Index based on performance criterion only evaluates the control error variance and does not consider the manipulating variable variance.

In the conventional performance-driven control system [12], controller parameters are calculated using closed-loop data to improve the generalized minimum variance index (GMV-Index), which considers controller error variance as well as manipulating variable variance. The scheme is based on the gradient method to avoid system identification. However, the calculation of control parameters for improving control performance takes considerable amount of time because of the gradient method.

This chapter proposes the following two new performance-driven control schemes in which the control parameters can be calculated without the use of

the gradient method.

(1) Performance-driven control system based on MV-index (PD-MVIndex) in section 3.2.

(2) Smart adaptive control system based on GMV-index (Smart-GMVIndex) in section 3.3.

In this chapter, a fictitious reference iterative tuning (FRIT) scheme [64] is utilized for calculating the controller parameters so that the control performance index (MV-Index and GMV-Index) is improved. FRIT is a practical data-driven tuning method and it can tune control parameters within only a single sampling interval. In PD-MVIndex control scheme, the application of 1-parameter tuning method is impossible because an adjustable parameter is not included in the controller parameters. In contrast, an adjustable parameter $\lambda$ (a weighting factor penalty of manipulating variable) is included in the Smart-GMVIndex control scheme.

## 3.2 Design of PD-MVIndex

### 3.2.1 System description

The controlled object can be expressed as follows:

$$A(z^{-1})y(t) = z^{-(k+1)}B(z^{-1})u(t) + \xi(t)/\Delta \tag{3.1}$$

$$\left.\begin{aligned} A(z^{-1}) &= 1 + a_1 z^{-1} + a_2 z^{-2} \\ B(z^{-1}) &= b_0 + b_1 z^{-1} + \cdots + b_m z^{-m} \end{aligned}\right\}, \tag{3.2}$$

where $y(t)$ is the system output, $u(t)$ is the control input, $k$ is the time-delay, $\xi(t)$ represents the Gaussian white noise with zero mean and covariance $\sigma^2$,

$z^{-1}$ is the back shift operator implying $z^{-1}y(t) = y(t-1)$, $\Delta$ is the difference operator ($\Delta := 1 - z^{-1}$), and $m$ is the order of $B(z^{-1})$. Note that the systems in Eq. (3.1) and Eq. (2.1) are different because the time-delay $k$ should be known to calculate MV-Index.

In this chapter, the PID controller is introduced as $C(z^{-1})/\Delta$ as follows:

$$u(t) = \frac{C(z^{-1})}{\Delta}\{r(t) - y(t)\} = \frac{C(z^{-1})}{\Delta}e(t) \tag{3.3}$$

$$C(z^{-1}) = k_c\Delta + \frac{k_c \cdot T_s}{T_I} + \frac{k_c \cdot T_D}{T_s}\Delta^2 \tag{3.4}$$

where $r(t)$ is the reference signal, $e(t)$ is the control error, $k_c$ is the proportional gain, $T_I$ is the reset time, $T_D$ is the derivative time, and $T_s$ is the sampling interval.

### 3.2.2 Control assessment index based on Minimum Variance control law: MV-Index

By referring to [63], the minimum variance control law based on the minimization of the following cost function is derived with respect to the system of Eq. (3.1).

$$J = \mathcal{E}\left[\phi^2(t+k+1)\right], \tag{3.5}$$

where $\mathcal{E}[\cdot]$ denotes the expectation. Accordingly, $\phi(t+k+1)$ represents an error between a system output and a reference model output. This error is provided as follows:

$$\phi(t+k+1) := P(z^{-1})y(t+k+1) - P(1)r(t) \tag{3.6}$$

A Diophantine equation given by Eq. (3.7) is then introduced.

$$P(z^{-1}) = \Delta A(z^{-1})E(z^{-1}) + z^{-(k+1)}F(z^{-1}) \tag{3.7}$$

$$E(z^{-1}) = 1 + e_1 z^{-1} + \cdots + e_k z^{-k} \tag{3.8}$$

$$F(z^{-1}) = f_0 + f_1 z^{-1} + f_2 z^{-2} \tag{3.9}$$

Subsequently, $P(z^{-1})$ is determined as a user-specified polynomial designed according to [11] and expressed as Eq. (2.8) provided in the previous chapter.

Eq. (3.6) can now be rewritten as follows (See Appendix 3.A):

$$\phi(t+k+1) = \frac{P(z^{-1})}{T(z^{-1})}\xi(t+k+1) \tag{3.10}$$

$$= E(z^{-1})\xi(t+k+1) + S(z^{-1})\xi(t) \tag{3.11}$$

$$T(z^{-1}) := \Delta A(z^{-1}) + z^{-(k+1)}B(z^{-1})C(z^{-1}) \tag{3.12}$$

$$S(z^{-1}) := \frac{F(z^{-1}) - B(z^{-1})C(z^{-1})E(z^{-1})}{T(z^{-1})}. \tag{3.13}$$

The cost function $J$ of Eq. (3.5) is then obtained using Eq. (3.11):

$$\begin{aligned} J &= \mathcal{E}\left[\phi^2(t+k+1)\right] \\ &= \mathcal{E}\left[\left\{E(z^{-1})\xi(t+k+1) + S(z^{-1})\xi(t)\right\}^2\right]. \end{aligned} \tag{3.14}$$

Eq. (3.14) can be separated as follows:

$$\begin{aligned} J &= \mathcal{E}\left[\left\{E(z^{-1})\xi(t+k+1)\right\}^2\right] \\ &\quad + \mathcal{E}\left[\left\{S(z^{-1})\xi(t)\right\}^2\right] \end{aligned} \tag{3.15}$$

$$= J_{\min} + J_0 \tag{3.16}$$

where

$$J_{\min} = \mathcal{E}\left[\left\{E(z^{-1})\xi(t+k+1)\right\}^2\right] \tag{3.17}$$

$$J_0 = \mathcal{E}\left[\left\{S(z^{-1})\xi(t)\right\}^2\right] \tag{3.18}$$

where $J_0 = 0$ when the optimal controller $C_{opt}(z^{-1})/\Delta$ is applied. In other words, the minimum variance is achieved when the cost function is $J = J_{\min}$.

The control performance assessment index (MV-Index) based on the minimum variance control law is defined as follows:

$$\kappa := \frac{J_{\min}}{J} = \frac{J_{\min}}{J_{\min} + J_0} = 1 - \frac{J_0}{J_{\min} + J_0} \tag{3.19}$$

The minimum variance is achieved when $J_0 = 0$. Furthermore, the MV-Index is assessed as a "good control" when $\kappa \to 1$ and as a "poor control" when $\kappa \to 0$.

The parameters of the polynomial $E(z^{-1})$ must be obtained to calculate $J_{\min}$ of Eq. (3.19). Hence, the method considered in [54] is introduced, according to which the control performance assessment index can be directly calculated from the closed-loop data.

The following equations are now discussed (See Appendix 3.B):

$$\phi(t) = \epsilon(t) + \sum_{i=0}^{M} \alpha_i \phi(t-k-i) \tag{3.20}$$

$$\epsilon(t) := E(z^{-1})\xi(t), \tag{3.21}$$

where $\alpha_i$ is an auto-regressive parameter, and $M$ is its order. The parameter $\alpha_i$ is identified using the least squares method. The following is obtained if

$N$ data are used for identification:

$$\mathbf{p(t)} = \mathbf{X(t)}\alpha\mathbf{(t)} + \mathbf{e(t)} \tag{3.22}$$

$$\mathbf{p(t)} := [\phi(t), \phi(t-1), \cdots, \phi(t-N+1)]^{\mathrm{T}} \tag{3.23}$$

$$\alpha = [\alpha_1, \alpha_2, \cdots, \alpha_M]^{\mathrm{T}} \tag{3.24}$$

$$\mathbf{e(t)} = [\epsilon(t), \epsilon(t-1), \cdots, \epsilon(t-N+1)]^{\mathrm{T}} \tag{3.25}$$

$$\mathbf{X(t)} = \begin{bmatrix} \phi(t-k-1) & \cdots & \phi(t-k-M) \\ \phi(t-k-2) & \cdots & \phi(t-k-M-1) \\ \vdots & \ddots & \vdots \\ \phi(t-k-N) & \cdots & \phi(t-k-M-N+1) \end{bmatrix} \tag{3.26}$$

Accordingly, parameter $\alpha(\mathbf{t})$ is calculated as follows:

$$\alpha(\mathbf{t}) = \{\mathbf{X(t)}^{\mathrm{T}}\mathbf{X(t)}\}^{-\mathbf{1}}\mathbf{X(t)}^{\mathrm{T}}\mathbf{p(t)} \tag{3.27}$$

Eq. (3.19) can now be provided as follows with sufficiently considerable amounts $N$ of data as the condition:

$$\kappa = \frac{\{\mathbf{p(t)} - \mathbf{X(t)}\alpha\mathbf{(t)}\}^{\mathrm{T}}\{\mathbf{p(t)} - \mathbf{X(t)}\alpha\mathbf{(t)}\}}{\mathbf{p(t)}^{\mathrm{T}}\mathbf{p(t)}} \tag{3.28}$$

### 3.2.3 Adjustment of PID parameters based on MV-Index using FRIT

FRIT [64] is a method used to directly calculate the control parameters of the controller by using the input and output data (i.e., $u_0(t)$ and $y_0(t)$) obtained from a single experiment and a fictitious reference signal (i.e., $\widetilde{r}(t)$) generated from these data. The FRIT proposed so far calculates a control parameter by using the data of a transient state. Meanwhile, the PD-MVIndex

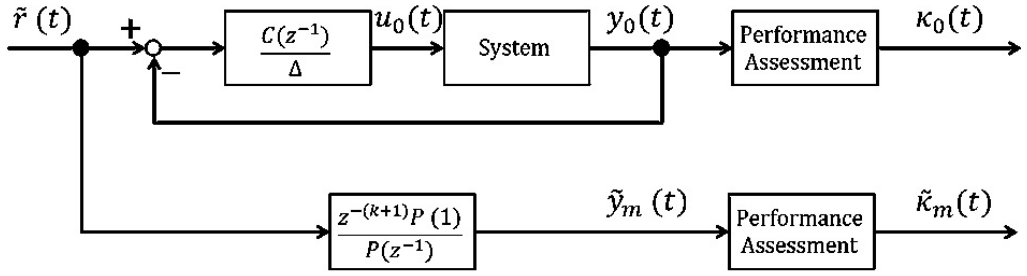


Figure 3.1: Block diagram of the FRIT method in PD-MVIndex control scheme.

control scheme using the FRIT method focuses on a steady state and considers the control performance assessment index $\kappa$, discussed in the previous section, in the FRIT calculation.

Figure 3.1 presents a block diagram of the FRIT in this PD-MVIndex control scheme. Based on Eq. (2.8), a desired reference model is considered in advance. The relational expression between the obtained input and output data (i.e., $u_0(t)$, and $y_0(t)$) and $C(z^{-1})$ is presented as follows:

$$u_0(t) = \frac{C(z^{-1})}{\Delta} \{\widetilde{r}(t) - y_0(t)\}. \tag{3.29}$$

The fictitious reference signal $\widetilde{r}(t)$ is calculated by using Eq. (3.29) as follows from the controller and the experiment data:

$$\widetilde{r}(t) = C(z^{-1})^{-1}\Delta u_0(t) + y_0(t). \tag{3.30}$$

Accordingly, the error $\phi_0(t)$ between output data and reference model output is calculated using the output data $y_0(t)$ by Eq. (3.6). The control performance assessment index $\kappa_0$ for a single experiment data is obtained using $\phi_0(t)$ by Eq. (3.28).

Similarly, let the output of a reference model with respect to the fictitious reference signal $\widetilde{r}(t)$ be $\widetilde{y}_m(t)$. A fictitious reference control error $\widetilde{\phi}_m(t)$ calculated from $\widetilde{y}_m(t)$ and $\widetilde{r}(t)$ is calculated using Eq. (3.6). Thus, the fictitious reference control performance assessment index $\widetilde{\kappa}_m$ is obtained through Eq. (3.28) using $\widetilde{\phi}_m(t)$.

The control parameters are determined through FRIT using the "fminsearch.m" of the OptimizationToolbox, MATLAB/Simulink Ver. 8.3.0.532 (R2014a), such that the absolute error between $\kappa_0$ and $\widetilde{\kappa}_m$ is minimized.

## 3.3 Design of smart-GMVIndex

### 3.3.1 Overview of the Smart-GMVIndex control system

In this section, the Smart-GMVIndex is proposed. Figure 3.2 shows the proposed Smart-GMVIndex control system, which consists of "control performance assessment" and "control design" modules.

In the "control performance assessment", the GMV-Index $\kappa_{\mathrm{GMV}}$ is calculated using closed-loop data without system model. The feature of GMV-Index is that it ranges between $0 \leq \kappa_{\mathrm{GMV}} \leq 1$, and $\kappa_{\mathrm{GMV}} = 0$ and $\kappa_{\mathrm{GMV}} = 1$ indicating poor and excellent control performances, respectively.

The control design part consists of "1-parameter tuning" and "controller redesign". Control parameters do not require to be tuned when the control performance is excellent. Therefore, "1-parameter tuning" works only when the control performance becomes good, and not excellent. In contrast, "controller redesign" works when the control performance becomes poor. The threshold $\alpha$ and $\beta$ are set in advance to define control performance as good

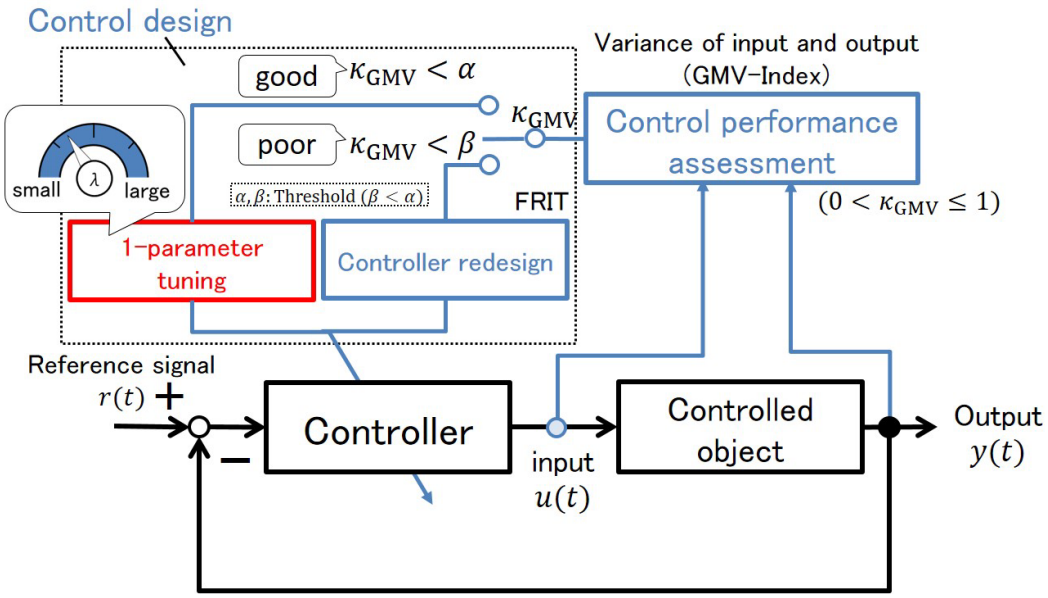


Figure 3.2: Schematic figure of the proposed Smart-GMVIndex control system.

or poor.

### 3.3.2 Control assessment index based on Generalized Minimum Variance control law: GMV-Index

The generalized minimum variance control law for the system in Eq. (3.1) can be derived by minimizing the following cost function [63]:

$$J = \mathcal{E}\left[\phi^2_{\mathrm{GMV}}(t+k+1)\right] \tag{3.31}$$

$$\phi_{\mathrm{GMV}}(t+k+1) := P(z^{-1})y(t+k+1) + \lambda\Delta u(t) - P(1)r(t), \tag{3.32}$$

where $\mathcal{E}[\cdot]$ denotes the expectation. In Eq. (3.32), $\lambda$ is a weighting factor penalty of control input.

Next, Eq. (3.32) can be re-expressed as follows by using Eqs. (3.1),

(3.3), and (3.7).

$$\phi_{\mathrm{GMV}}(t+k+1) = \frac{P(z^{-1})}{T(z^{-1})}\xi(t+k+1) - \frac{\lambda C(z^{-1})}{T(z^{-1})}\xi(t) \tag{3.33}$$

$$= E(z^{-1})\xi(t+k+1) + S_{\mathrm{GMV}}(z^{-1})\xi(t) \tag{3.34}$$

$$S_{\mathrm{GMV}}(z^{-1}) := \frac{F(z^{-1}) - B(z^{-1})C(z^{-1})E(z^{-1}) - \lambda C(z^{-1})}{T(z^{-1})} \tag{3.35}$$

In addition, Eq. (3.8) indicates that $E(z^{-1})$ is of the $k$ order. $E(z^{-1})\xi(t+k+1)$ of Eq. (3.34) is a signal generated after time $t$. Hence, $E(z^{-1})\xi(t+k+1)$ cannot be obtained at time $t$. Accordingly, $C(z^{-1})$ of Eq. (3.35) is designed so that $S(z^{-1})$ of Eq. (3.34) becomes zero. The $C_{opt}(z^{-1})$ included in the optimal controller $C_{opt}(z^{-1})/\Delta$ is calculated as follows:

$$C_{\mathrm{opt}}(z^{-1}) = \frac{F(z^{-1})}{G(z^{-1}) + \lambda} \tag{3.36}$$

$$G(z^{-1}) := E(z^{-1})B(z^{-1}). \tag{3.37}$$

The following equation is obtained by replacing the steady-state term $G(1)$ with the polynomial $G(z^{-1})$ in Eq. (3.36) to design PID controller.

$$C(z^{-1}) = \frac{f_0 + f_1 z^{-1} + f_2 z^{-2}}{G(1) + \lambda} \tag{3.38}$$

The PID paraemters can approximately be replaced by $F(z^{-1})$ and $G(1)$ as follows by comperaing the coefficients of Eq. (3.4) and (3.38):

$$\left.\begin{aligned} k_c &= -\frac{f_1 + 2f_2}{G(1) + \lambda} \\ T_I &= -\frac{f_1 + 2f_2}{f_0 + f_1 + f_2} T_s \\ T_D &= -\frac{f_2}{f_1 + 2f_2} T_s \end{aligned}\right\}. \tag{3.39}$$

### 3.3.3 Controller performance index based on GMVC

$\kappa_{\mathrm{GMV}}$ can be calculated by Eq. (3.28), and note that $\phi_{\mathrm{GMV}}(t)$ is utilized instead of $\phi(t)$ when $\kappa_{\mathrm{GMV}}$ is obtained.

### 3.3.4 Adjustment of PID parameters based on GMV-Index using FRIT

In this section, the "Control redesign" module in Figure 3.2 is described. First, the user-specified thresholds $\alpha$ and $\beta$ ($\alpha > \beta$) are set in advance to judge the control performance as "excellent" or "good" or "poor". Specifically, the "Controller redesign" works when $\kappa < \beta$ (control performance becomes poor), and "1-parameter tuning" works when $\kappa < \alpha$ (control performance becomes good, and not excellent). In section 3.3.5, the tuning of all the control parameters by using FRIT in the "Controller redesign" module is explained. Moreover, section 3.3.6, describes the "1-parameter tuning" by adjusting $\lambda$ based on the trade-off curve.

### 3.3.5 Fictitious reference iterative control scheme

A performance-driven control scheme based on GMV-Index [63] has been proposed; however, it takes a considerable amounts of time to tune control parameters when control performance becomes poor due to the use of a gradient method. Thus, the FRIT scheme [64] is introduced in this section.

Figure 3.3 shows a block diagram of the proposed FRIT. Firstly, the user-specified reference model is given in Eq. (2.8) in advance. In Figure 3.3, control parameters of $C(z^{-1})$ can be calculated without a system model by

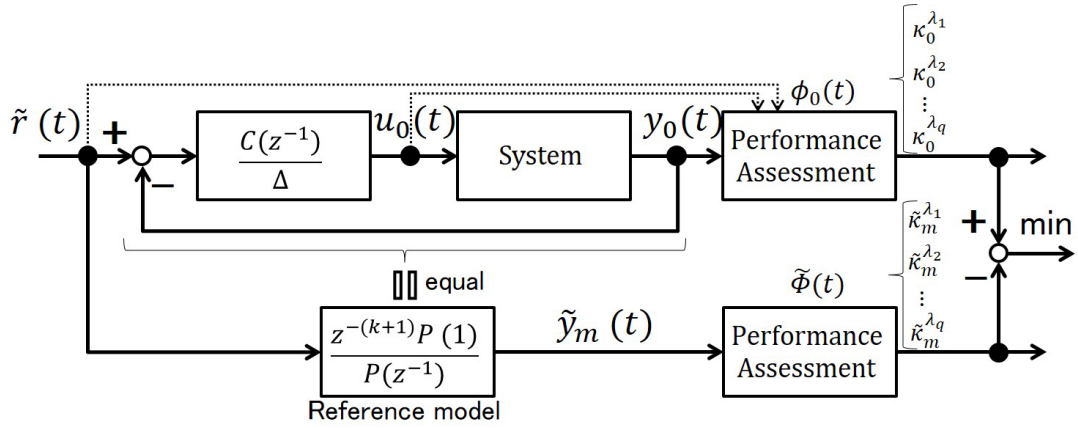


Figure 3.3: Block diagram of FRIT in smart-GMVIndex control scheme.

using closed loop data (input $u_0(t)$ and output $y_0(t)$) so that the following cost function is minimized.

$$J_{\mathrm{FRIT}} = \sum_{i=1}^{q} \left(\kappa_0^{\lambda_i} - \widetilde{\kappa}_m^{\lambda_i}\right)^2, \tag{3.40}$$

where $q$ is the nonnegative integer ($q \geq 0$), $\lambda_i$ is the variable of $\lambda$ ($\lambda_i \geq 0$), $\kappa_0^{\lambda_i}$ is the GMV-Index for each $\lambda_i$ obtained by using $u_0(t)$ and $y_0(t)$ in Eqs. (3.32) and (3.28) respectively, and $\widetilde{\kappa}_m^{\lambda_i}$ is the fictitious GMV-Index for each $\lambda_i$. The feature of the proposed FRIT is that some GMV-Indexes can be calculated for each $\lambda_i$ by using the same set of closed-loop data.

Here, the fictitious GMV-Index $\widetilde{\kappa}_m^{\lambda_i}$ is calculated using a fictitious reference input $\widetilde{r}(t)$ and fictitious reference output $\widetilde{y}(t)$ in chapter 3.2.3.

The desired control performance can be obtained by optimizing controller $C(z^{-1})$ so that Eq. (3.40) is minimized. For instance, the optimal $C(z^{-1})$ is obtained using the genetic algorithm or the optimal tool box in Matlab. Specifically, the four parameters $f_1 + 2f_2$, $G(1)$, $T_I$, and $T_D$ of $C(z^{-1})$ in Eq. (3.39) are optimized.

The proposed FRIT tuning algorithm is summarized as follows.

(1) Obtain a closed-loop data $u_0(t)$ and $y_0(t)$.

(2) Design $P(z^{-1})$ and $\lambda_i$.

(3) Calculate $\kappa_0^{\lambda_i}$ for each $\lambda_i$ by using $u_0(t)$ and $y_0(t)$.

(4) Calculate $\widetilde{u}_m(t)$ and $\widetilde{y}_m(t)$ by using $u_0(t)$ and $y_0(t)$, respectively.

(5) Calculate $\widetilde{\kappa}_0^{\lambda_i}$ for each $\lambda_i$ by using $\widetilde{u}_m(t)$ and $\widetilde{y}_m(t)$.

(6) Optimize $f_1+2f_2$, $G(1)$, $T_I$, and $T_D$ of $C(z^{-1})$ to minimize Eq. (3.40).

### 3.3.6 1-parameter tuning based on GMV-Index

In [12], the trade-off curve in Figure 3.4 has been discussed. The trade-off curve indicates the relationship between $\lambda$ and variance of $e(t)$ and $\Delta u(t)$. Therefore, it is utilized in the 1-parameter tuning. The variance of $e(t)$ and $\Delta u(t)$ can be expressed by using $H2$-norm $||\cdot||_2$ as follows [12]:

$$\mathcal{E}[e^2(t)] = \left|\left|-\frac{1}{T(z^{-1})}\right|\right|_2^2 \sigma_\xi^2 \tag{3.41}$$

$$\mathcal{E}[\{\Delta u(t)\}^2] = \left|\left|-\frac{C(z^{-1})}{T(z^{-1})}\right|\right|_2^2 \sigma_\xi^2, \tag{3.42}$$

where

$$T(z^{-1}) := \Delta\widetilde{A}(z^{-1}) + z^{-(k+1)}\widetilde{B}(z^{-1})C(z^{-1}). \tag{3.43}$$

In Eqs. (3.41) and (3.42), $\sigma_\xi^2$ shows the covariance of Gaussian white noise. In addition, $\widetilde{A}(z^{-1})$ and $\widetilde{B}(z^{-1})$ are the polynomials of a discrete-time model

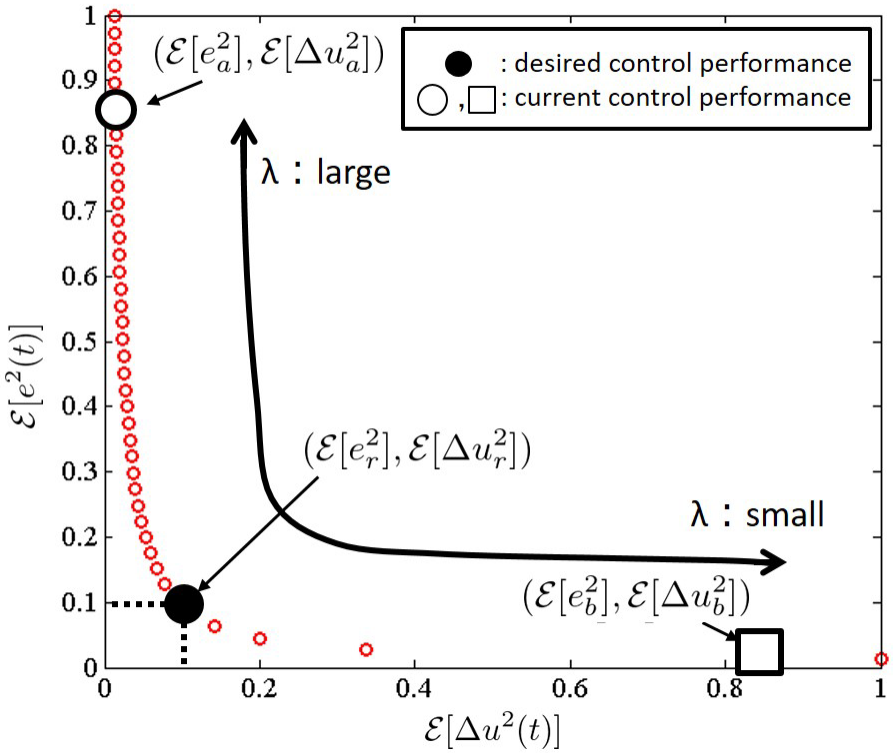


Figure 3.4: Tradae-off curve indicated by changing $\lambda$.

corresponding to Eq. (3.1) and are described as follows:

$$\widetilde{A}(z^{-1})y(t) = z^{-(k+1)}\widetilde{B}(z^{-1})u(t) + \xi(t)/\Delta \tag{3.44}$$

$$\left.\begin{aligned} \widetilde{A}(z^{-1}) &= 1 + \widetilde{a}_1 z^{-1} + \widetilde{a}_2 z^{-2} \\ \widetilde{B}(z^{-1}) &= \widetilde{b}_0 + \widetilde{b}_1 z^{-1} + \cdots + \widetilde{b}_{\widetilde{m}} z^{-\widetilde{m}} \end{aligned}\right\}, \tag{3.45}$$

where $\widetilde{m}$ is the order of $\widetilde{B}(z^{-1})$. The system identification is required in order to obtain the trade-off curve.

After obtaining the trade-off curve by using Eqs. (3.41) and (3.42), the desired control performance (point "•" in Figure 3.4) is set. Then, $\lambda$ can be chosen by the trade-off curve, indicating that $k_c$ is calculated from $\lambda$, $f_1 + f_2$, and $G(1)$ in Eq. (3.39). Collectively, the calculation of $T_I$ and $T_D$ is shown

in section 3.3.5, and that of $k_c$ is shown in section 3.3.6.

Next, the 1-parameter tuning by the adjusting of $\lambda$ is described. First, the following criterion $J_r$ is defined:

$$J_r = \frac{\mathcal{E}[e_r^2]}{\mathcal{E}[\Delta u_r^2]}. \tag{3.46}$$

Second, the current criterion $J(t)$ is calculated as

$$J(t) = \frac{\mathcal{E}[e^2(t)]}{\mathcal{E}[\Delta u^2(t)]}. \tag{3.47}$$

Then, (i) $\lambda$ is increased when $J_r > J(t)$ or (ii) $\lambda$ is decreased when $J_r < J(t)$.

For example, if the current control performance is at the point "$\circ$" in Figure 3.4, the current criterion $J(t)$ is calculated as $J(t) = \mathcal{E}[e_a^2]/\mathcal{E}[\Delta u_a^2]$. Furthermore, $\lambda$ is decreased because $J_r < J(t)$ to go to the point "$\bullet$" from "$\circ$". However, if the current control performance is the pont "$\square$", $J(t) = \mathcal{E}[e_b^2]/\mathcal{E}[\Delta u_b^2]$ and it is smaller than $J_r$. Therefore, $\lambda$ is increased.

Note that $\lambda$ of GMV-Index is constant even though $k_c$ is adjusted through 1-parameter tuning. However, $\lambda$ of GMV-Index is reset when all control parameters are recalculated.

## 3.4 Numerical example

### 3.4.1 Application of PD-MVIndex controller

[Time-invariant system]

The effectiveness of PD-MVIndex control scheme is verified using a numerical example. Table 3.1 presents the user-specified parameters in PD-MVIndex control scheme using the FRIT method. Table 3.2 lists the specifications of the computer used for this simulation.

Table 3.1: User-specified parameters in the numerical simulation of PD-MVIndex controll scheme.

| | |
|---|---|
| $r$: target value | 5 |
| $\sigma$: coefficient regarding the rise characteristic | 40 |
| $\delta$: coefficient regarding the decay characteristic | 0 |
| $N$: number of data | 1000 |
| $M$: auto-regressive parameter order | 20 |

Table 3.2: Performance of the computer used for the numerical simulation.

| | |
|---|---|
| Processor | Intel(R) Core(TM) i7-4770 CPU 3.4GHz |
| System type | 64-bit operating system |
| Memory | 16.0GB |
| OS | Windows 8.1 |

A controlled object is given as the following "first order lag + time-delay" system:

$$G(s) = \frac{10}{1+100s}e^{-8s}. \tag{3.48}$$

The system parameter included in Eq. (3.1) is obtained as follows by discretizing Eq. (3.48) with the sampling time $T_s = 10$ [s]:

$$A(z^{-1})y(t) = z^{-1}B(z^{-1})u(t) + \xi(t)/\Delta \tag{3.49}$$

$$\left.\begin{aligned} A(z^{-1}) &= 1 - 0.905z^{-1} \\ B(z^{-1}) &= 0.198 + 0.754z^{-1} \end{aligned}\right\}. \tag{3.50}$$

The white Gaussian noise $\xi(t)$ is set at a zero mean and the variance is $0.01^2$. The following PID gains are applied as initial parameters:

$$K_P = 0.75, \quad K_I = 0.02, \quad K_D = 0.75 \tag{3.51}$$

Figure 3.5 shows the control result obtained using the fixed PID parameters to demonstrate the effectiveness of the PD-MVIndex scheme. Figure 3.6

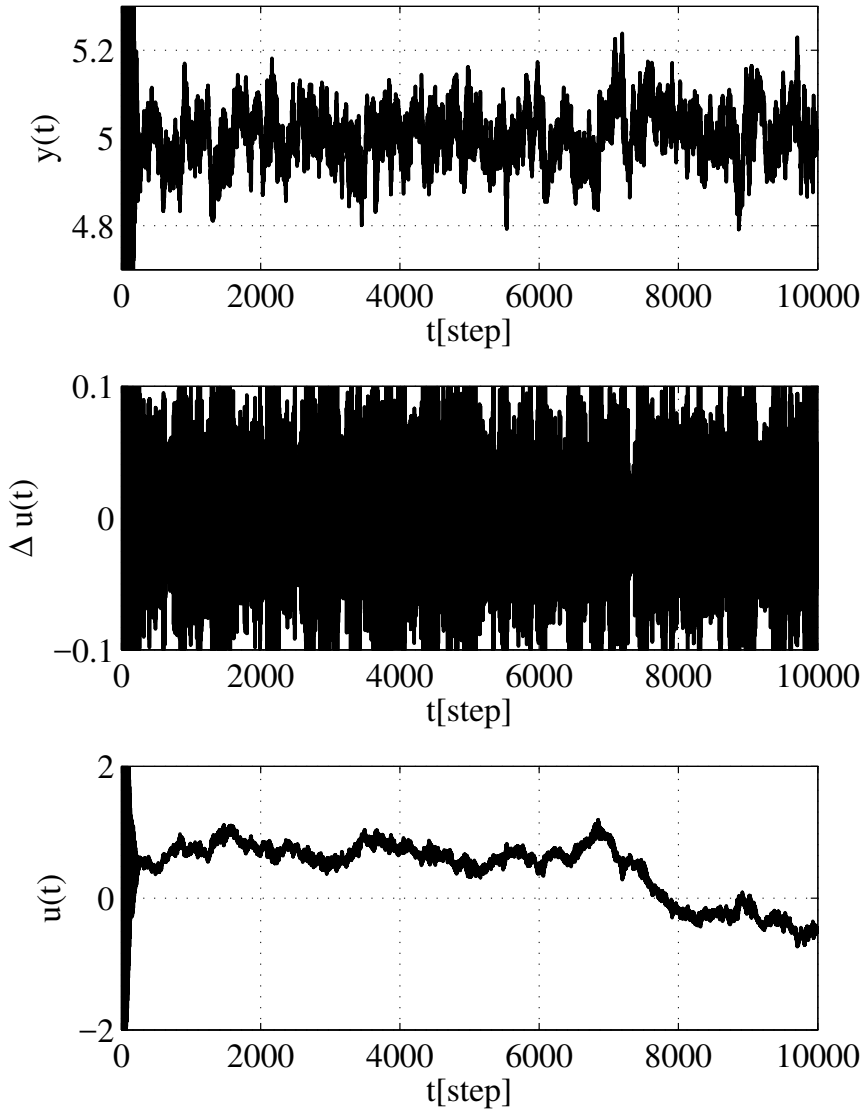


Figure 3.5: Control result obtained using the fixed PID control ($K_P = 0.75, K_I = 0.02$, and $K_D = 0.75$).

shows the trajectory of the control performance assessment index, $\kappa$ corresponding to Figure 3.5. The figure shows that $\kappa$ is calculated after 2000 [step] because the control performance in the steady state is assessed. The relation-

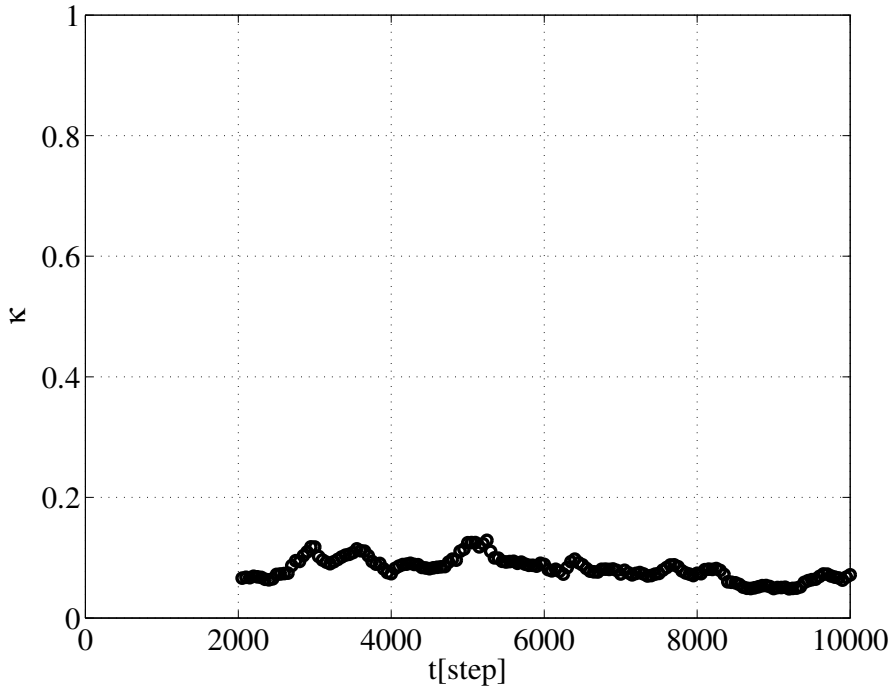


Figure 3.6: Trajectory of $\kappa$ corresponding to Figure 3.5.

ship expressed in Eq. (3.19) shows that the value of $\kappa$ is close to 0 in Figure 3.6. Therefore, the PID gains of Eq. (3.51) need to be re-tuned.

Figure 3.7 shows a control result obtained using the proposed PD-MVIndex control scheme and the FRIT method. Figure 3.8 shows the trajectory of the control performance assessment index $\kappa$. Figure 3.9 demonstrates a trajectories of PID gains, where the initial PID gains are the same as in Eq. (3.51). The calculation of the control performance assessment index and the PID gains adjustment at 3000 [step] are performed at the same step. More specifically, the control performance assessment index $\kappa$ was calculated using the input and output data for 1000 [step] from 2000 [step] to 2999 [step]. In addition, the PID gains of the following equation are calculated using the

PD-MVIndex control scheme. Note that the "assessment" and the "design" in this method are integrated.

$$K_P = 0.43, \quad K_I = 0.11, \quad K_D = 0.01 \tag{3.52}$$

The difference between $\kappa_0$ and $\widetilde{\kappa}_m$ calculated using "fminsearch.m" in the PID gains calculation of the above mentioned equation is $1.62 \times 10^{-6}$. The offline calculation time in the computer at this time is 0.75 [s] (Table 3.2). Although MATLAB is used, the calculation is completed within a specific time in the case of a relatively long sampling time (e.g., process systems).

Figure 3.7 indicates that the input and output variance is suppressed after adjusting the PID gains. In addition, Figure 3.8 shows that the control performance significantly improved. These results verify the effectiveness of the PID gains calculation based on the MV-Index from the closed-loop data.

Figure 3.8 shows the improvement of the control performance for 1000 [step] from 3000 [step] to 4000 [step] caused by the amount of data for $\kappa$ calculation (Table 3.1) $N = 1000$. Hence, the smaller the number of data, the faster the rise of $\kappa$ in Figure 3.8 and the greater the variance of $\kappa$.

The control results of the conventional scheme (i.e., the scheme using the gradient method) by proposed in [63], which is an online adjustment method, are presented in Figures 3.10-3.12. The control parameters in the gradient method of the conventional scheme were adjusted using the following equation, such that the control performance assessment index $\kappa$ was improved:

$$\mathbf{K(t)} = \mathbf{K(t-k)} - \eta \frac{\partial \kappa(\mathbf{t})}{\partial \mathbf{K(t-k)}} \tag{3.53}$$

$$\mathbf{K(t)} = [K_P(t), K_I(t), K_D(t)]^T \tag{3.54}$$

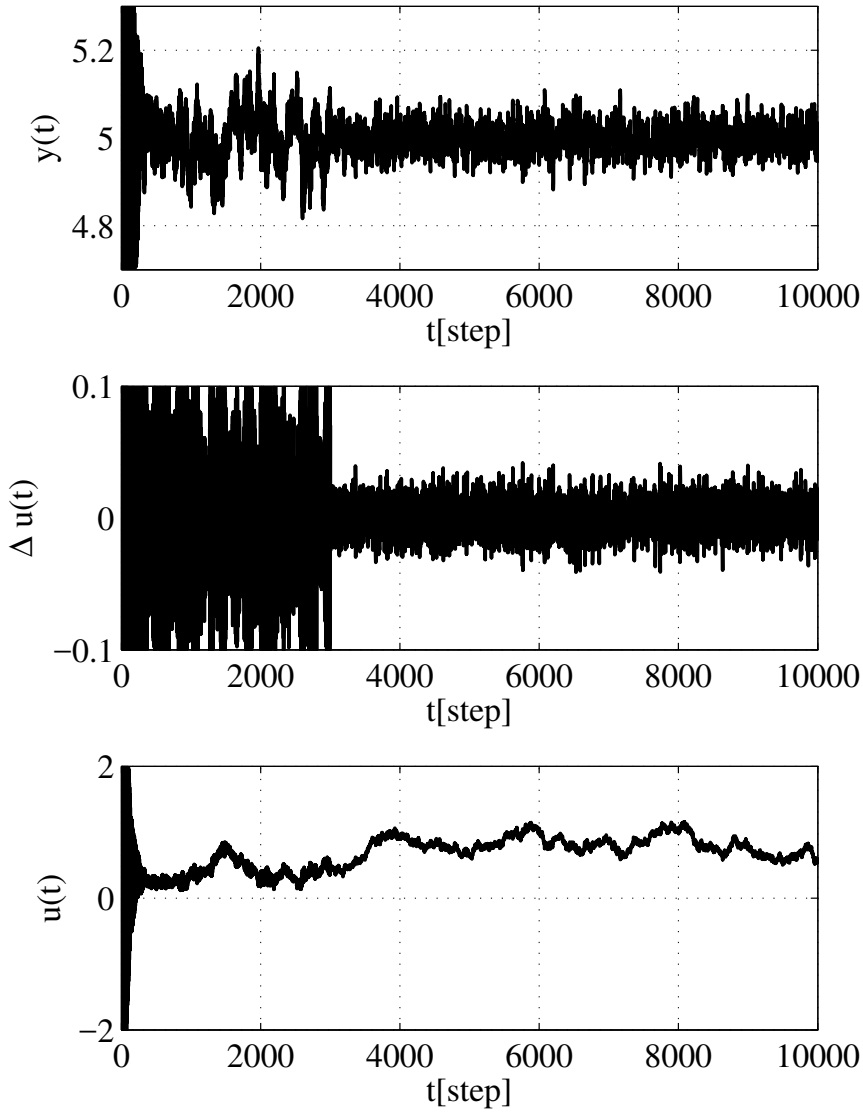


Figure 3.7: Control result by the proposed PD-MVIndex control using the FRIT method.

where, $\eta$ represents the learning coefficient of each PID gains, which is set to 0.02.

Figures 3.7 and 3.10 show that after 3000 [steps] from the initiation of

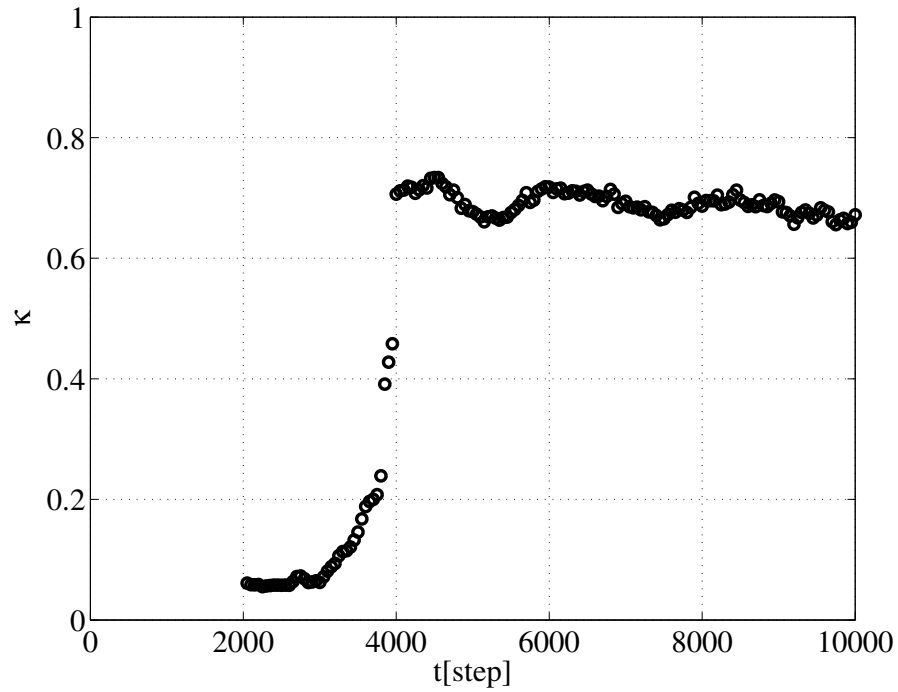


Figure 3.8: Trajectory of $\kappa$ corresponding to Figure 3.7.

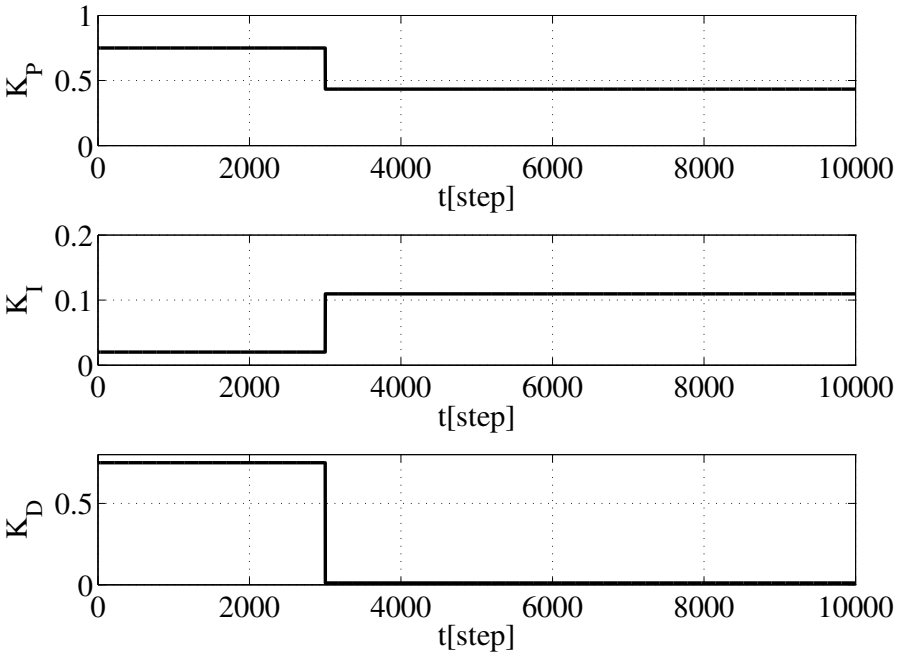


Figure 3.9: Trajectories of the PID gains corresponding to Figure 3.7.

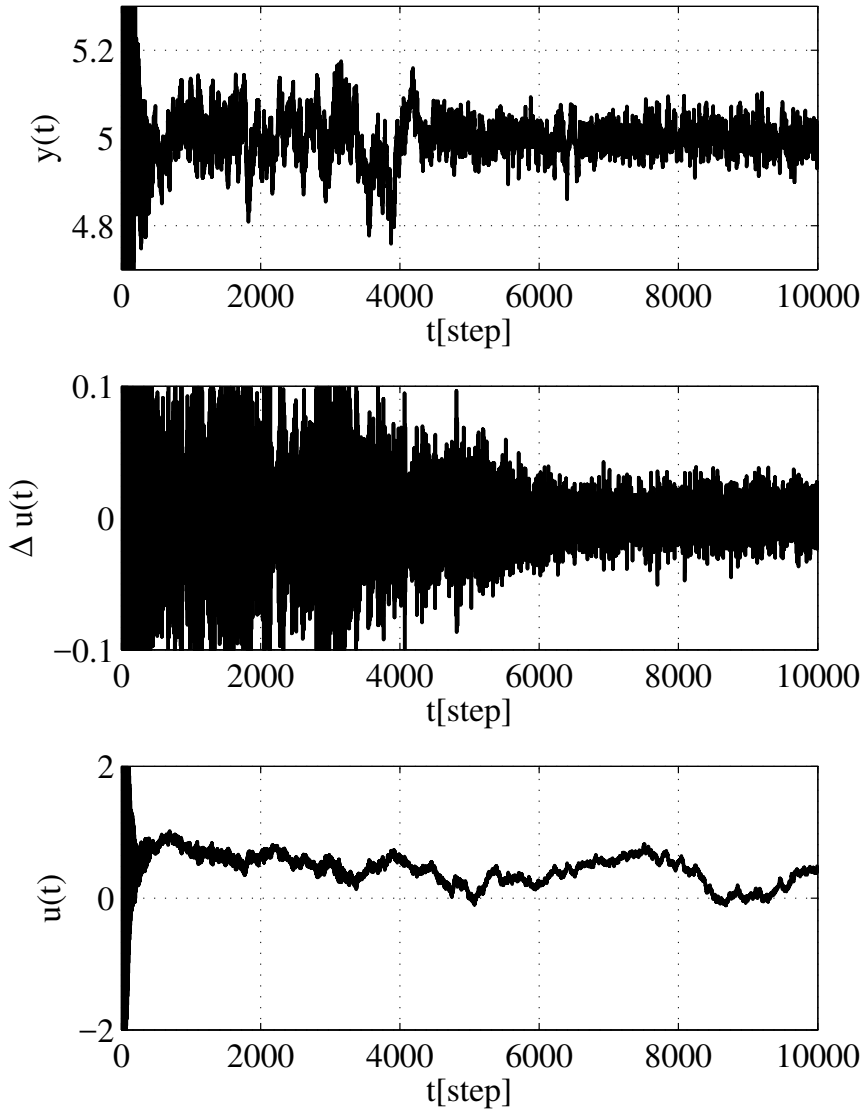


Figure 3.10: Control result of the conventional scheme (online learning [63] by using the gradient method).

the PID gains adjustment, the input and output variance in the conventional scheme gradually reduces because of the use of the gradient method. Furthermore, the improvement of the control performance takes time. This result is

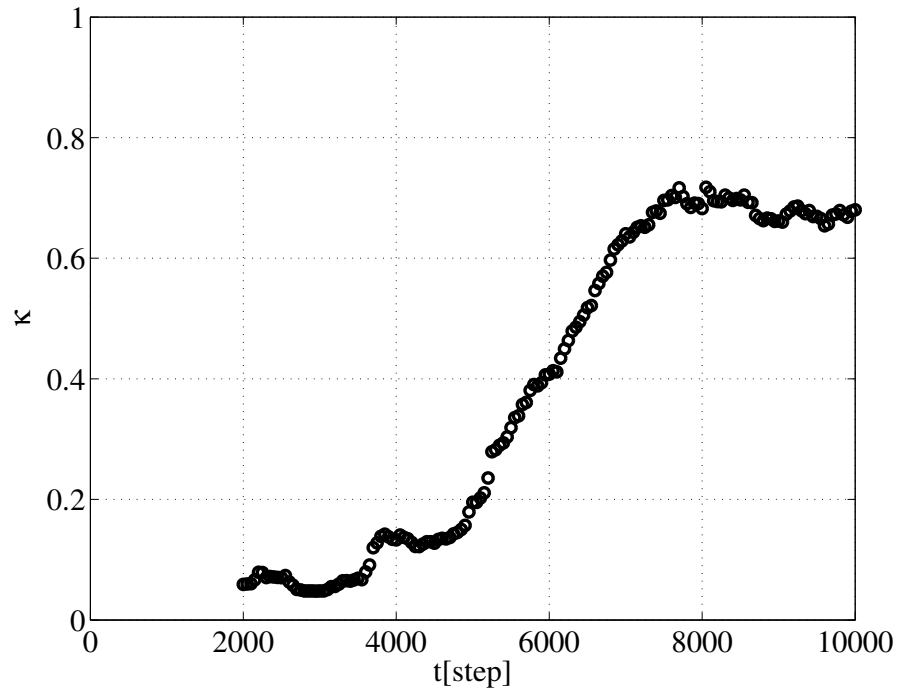


Figure 3.11: Trajectory of $\kappa$ corresponding to Figure 3.10.

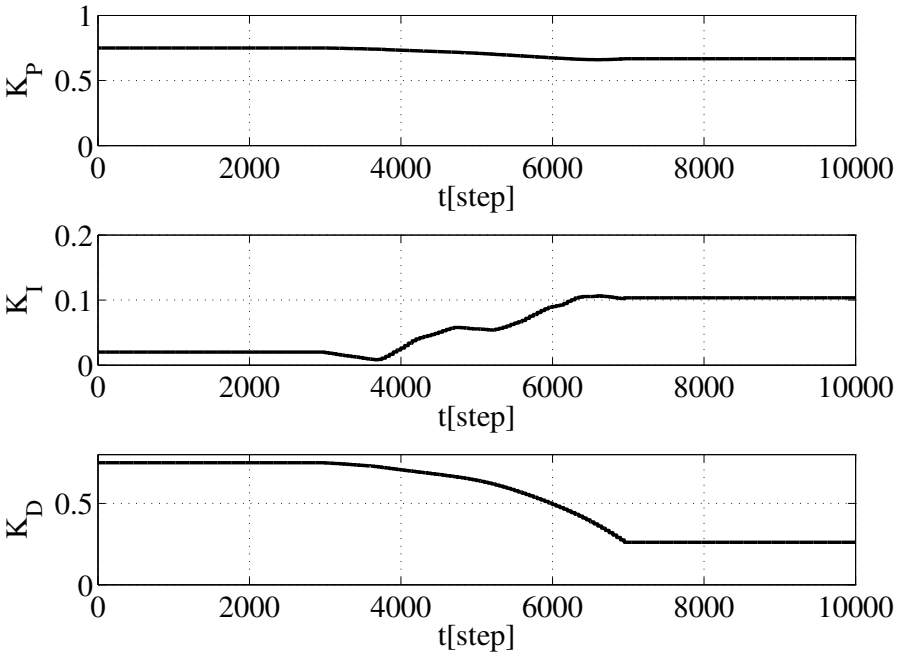


Figure 3.12: Trajectories of the PID gains corresponding to Figure 3.10.

also confirmed with the trajectory of $\kappa$ in Figure 3.11, where $\kappa$ gradually improves after 3000 [step]. Figure 3.12 shows a transition of the PID gain of the online adjustment method using the gradient method. A single adjustment of PID gains alone sufficiently improves the control performance in the proposed PD-MVIndex control scheme shown in Figure 3.9. However, in Figure 3.12, the adjustment width of the PID gains in the conventional scheme reduces because of the use of the gradient method.

[Time-variant system]

Next, the effectiveness of the proposed PD-MVIndex control scheme is verified by a time-variant system. The following first-order system with time-delay is introduced.

$$G(s) = \frac{K}{1+Ts} e^{-8s}, \tag{3.55}$$

where $T$ and $K$ are the system gain and time constant, respectively. In this numerical example, Eq. (3.55) is a time-variant system in which $T$ and $K$ are changed as follows:

$$T = \begin{cases} 100 & (0 \leq t \leq 5000) \\ 100 - \dfrac{30(t-5000)}{2500} & (5000 < t \leq 7500) \\ 70 & (7500 < t \leq 10000) \end{cases} \tag{3.56}$$

$$K = \begin{cases} 10 & (0 \leq t \leq 5000) \\ 10 + \dfrac{12(t-5000)}{2500} & (5000 < t \leq 7500) \\ 22 & (7500 < t \leq 10000) \end{cases} . \tag{3.57}$$

The following sets of PID parameters are obtained by using the ZN

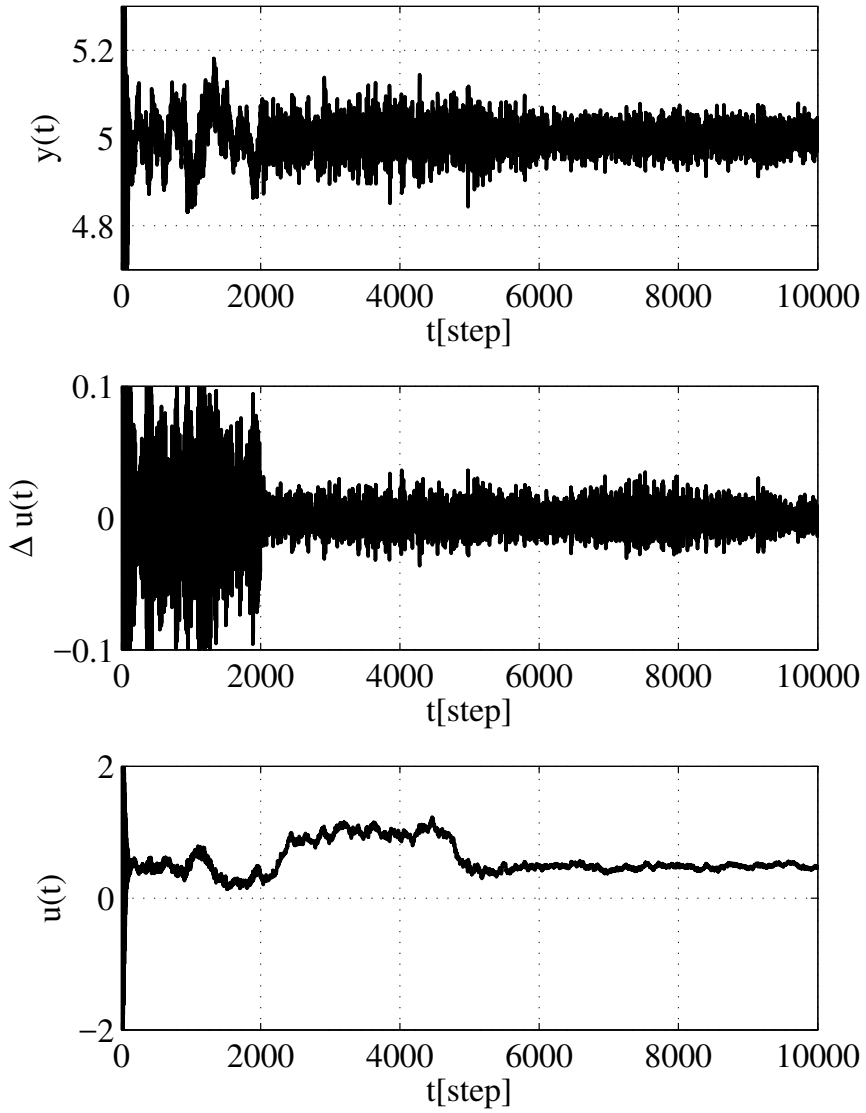


Figure 3.13: Control result obtained using the conventional scheme (online learning [63] by using the gradient method).

method [46] from the initial closed-loop data of Eq. (3.55).

$$k_c = 0.75, \quad T_I = 375, \quad T_D = 9.33 \tag{3.58}$$

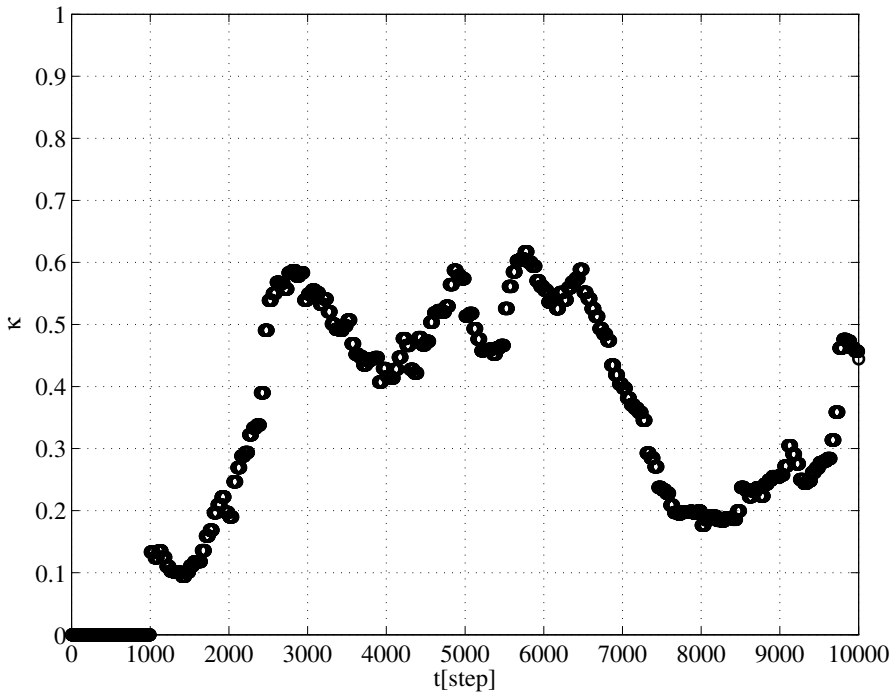


Figure 3.14: Trajectory of $\kappa$ corresponding to Figure 3.13.

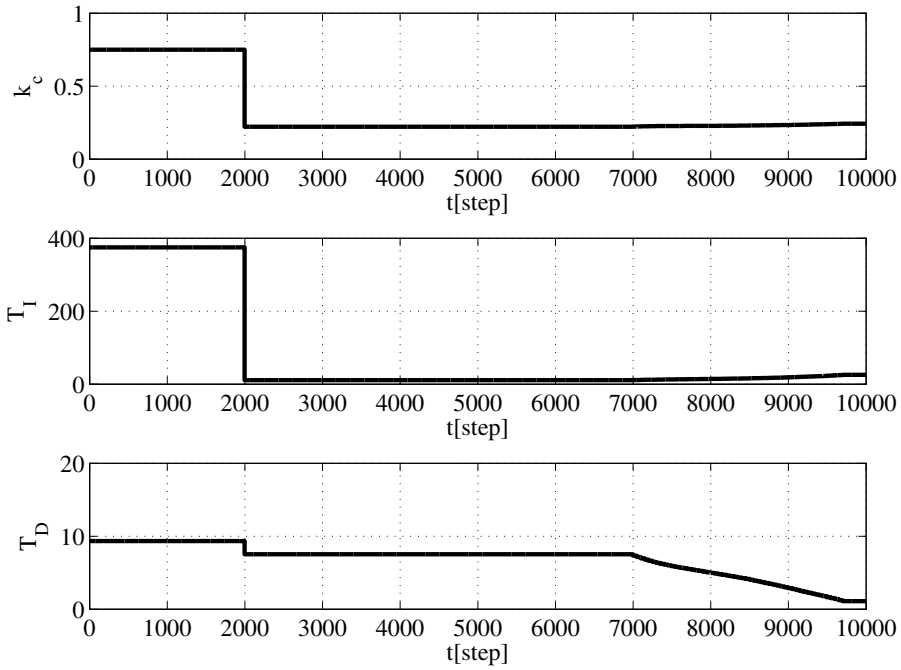


Figure 3.15: Trajectories of the PID parameters corresponding to Figure 3.13.

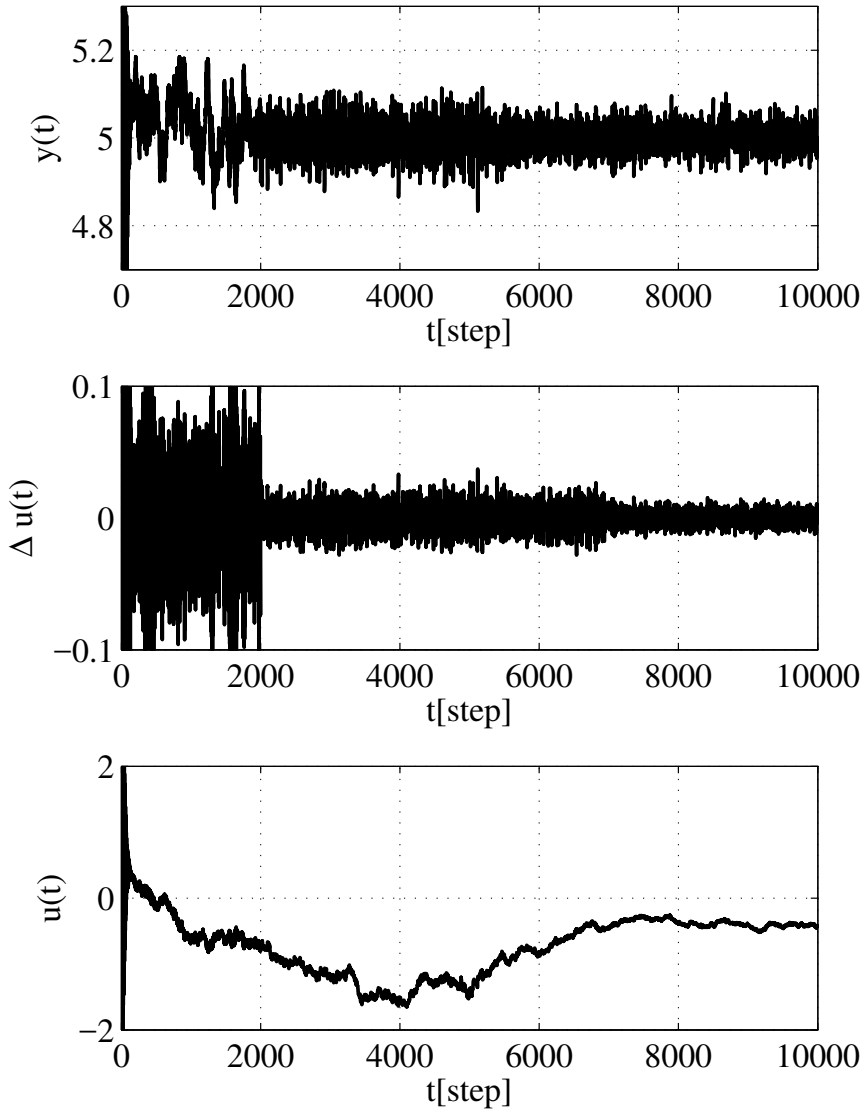


Figure 3.16: Control result by the proposed PD-MVIndex control using the FRIT method.

The numerical simulation was performed for the discrete time model Eq. (3.1) obtained by the discretization of Eq. (3.55).

First, Figure 3.13 shows a control result obtained using conventional

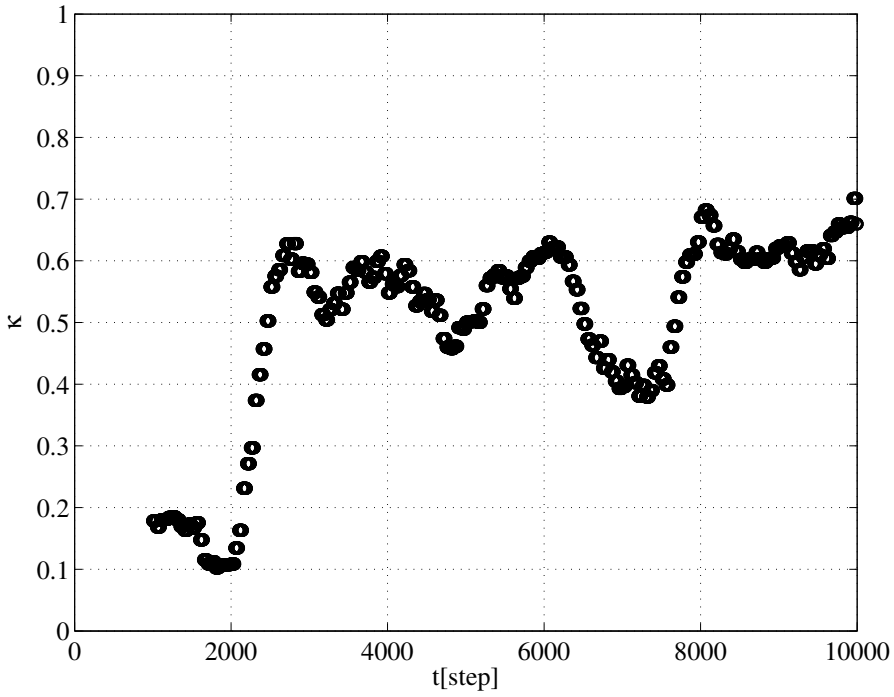


Figure 3.17: Trajectory of $\kappa$ corresponding to Figure 3.16.

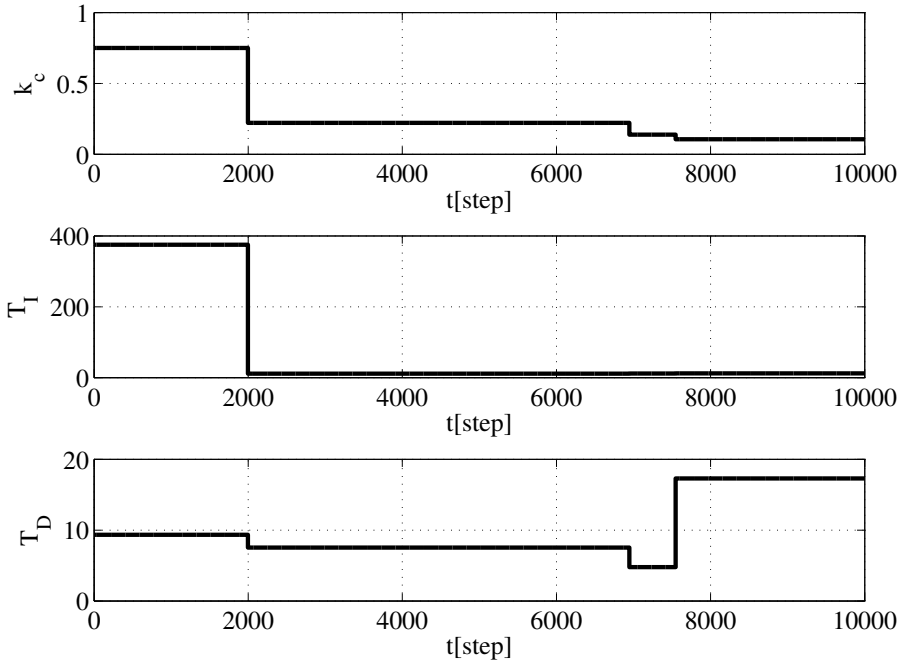


Figure 3.18: Trajectories of the PID gains corresponding to Figure 3.16.

scheme in which PID parameters are tuned using gradient method. Moreover, Figures 3.14 and 3.15 respectively show the trajectory of $\kappa$ and PID parameters corresponding to Figure 3.13. PID parameters are tuned using the gradient method to improve the control performance index $\kappa$. Each of $\eta$ in Eq. (3.53) is set to 0.005. The gradient method is conducted when $\kappa$ deteriorates to below 0.4. PID parameters are adjusted after 7000[step], however; the improvement speed of $\kappa$ is slow because the conventional scheme is based on the gradient method.

Next, Figure 3.16 shows the control result of the proposed scheme. Furthermore, Figures 3.17 and 3.18 respectively show the trajectory of $\kappa$ and PID parameters corresponding to Figure 3.16. Figure 3.18 shows that the PID parameters are tuned because $\kappa$ is smaller than 0.4 around 7000[step] in Figure 3.17. The speed of improving $\kappa$ in Figure 3.17 is faster than in the conventional scheme one shown in Figure 3.14. Thus, the effectiveness of the proposed scheme is verified in the time-variant system.

### 3.4.2 Application of Smart-GMVIndex controller

The effectiveness of the proposed Smart-GMVIndex control scheme is verified using a numerical example. The user-specified parameters in Smart-GMVIndex control scheme are set as $r = 5, \sigma = 75, \delta = 0, N = 1000, M = 20, \alpha = 0.3$, and $\beta = 0.1$. A controlled object is represented by the first oder system with a time delay as described in Eq. (3.55). $T, K$, and $L$ of Eq. (3.55) are set as $T = 100, K = 10$, and $L = 50$.

The system parameter included in Eq. (3.1) is obtained as follows by

discretizing the above mentioned controlled object with the sampling time $T_s = 10$ [s]:

$$A(z^{-1})y(t) = z^{-6}B(z^{-1})u(t) + \xi(t)/\Delta \tag{3.59}$$

$$\left.\begin{aligned} A(z^{-1}) &= 1 - 0.905z^{-1} \\ B(z^{-1}) &= 0.9516 \end{aligned}\right\} \tag{3.60}$$

Now, let the white Gaussian noise $\xi(t)$ be a zero mean and the variance be $0.01^2$. In the proposed Smart-GMVIndex control scheme, closed-loop data is needed to calculate PID gains in advance. Therefore, the following PID gains are applied as initial parameters to obtain the initial closed-loop data:

$$k_c = 0.24, \quad T_I = 200.0, \quad T_D = 30.0. \tag{3.61}$$

The GMV-Index $\kappa_{\mathrm{GMV}}$ of the initial closed-loop data is calculated using Eq. (3.61) as 0.17. Next, PID parameters of the proposed scheme are calculated using the initial closed-loop data. $\lambda$ is chosen as 0.5 from the trade-off curve when a desired variance of $e(t)$ is set as 0.03. The PID parameters are calculated using the proposed scheme as follows:

$$k_c = 0.19, \quad T_I = 190.7, \quad T_D = 32.8. \tag{3.62}$$

The GMV-Index $\kappa_{\mathrm{GMV}}$ of the proposed scheme using Eq. (3.62) is calculated as 0.45, and is improved from the initial closed-loop data($\kappa_{\mathrm{GMV}} = 0.17$). Furthermore, a variance of $e(t)$ is 0.025 and the desired variance of $e(t)$ (0.03) is satisfied.

To verify the effectiveness of the proposed scheme, system parameters

are changed as follows:

$$T = \begin{cases} 100 & (0 \leq t \leq 3000) \\ 100 - \dfrac{50(t-300)}{3000} & (3000 < t \leq 7000) \\ 50 & (7000 < t \leq 10000) \end{cases} \tag{3.63}$$

$$K = \begin{cases} 10 & (0 \leq t \leq 3000) \\ 10 + \dfrac{10(t-300)}{3000} & (3000 < t \leq 7000) \\ 20 & (7000 < t \leq 10000) \end{cases} . \tag{3.64}$$

Figure 3.19 shows a control result obtained using the fixed PID parameters to demonstrate the effectiveness of the proposed scheme. Figure 3.20 shows the trajectory of the control performance assessment index, $\kappa_{\mathrm{GMV}}$. The figure shows that $\kappa_{\mathrm{GMV}}$ is calculated after the 2000 [step] because the control performance in the steady state is assessed. The control performance is poor because $\kappa_{\mathrm{GMV}}$ is close to 0. Therefore, the PID gains of Eq. (3.62) must be be retuned.

Figure 3.21 shows a control result obtained using the proposed scheme, and it is better than that in Figure 3.19. Moreover, Figure 3.22 shows the trajectory of the GMV-Index $\kappa_{\mathrm{GMV}}$, which is improved after 3900[step] by using 1-parameter tuning when $\kappa_{\mathrm{GMV}}$ is less than $\alpha = 0.3$. However, the system parameters are changed as shown in Eqs.(3.63) and (3.64), and $\kappa_{\mathrm{GMV}}$ is smaller than $\beta = 0.1$ at approximately the 6500[step]. Therefore, all the PID parameters are retuned through controller redesign at approximately the 6500[step]. Figure 3.23 shows the trajectories of PID gains. Only $k_c$ is tuned through 1-parameter tuning between 3900[step] to 6500[step] in Figure

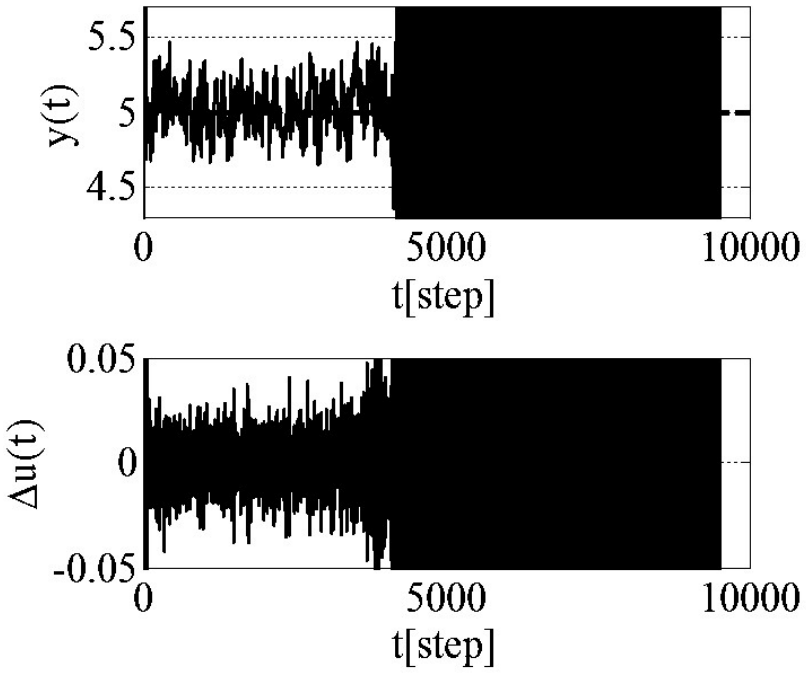


Figure 3.19: Control result by using the fixed PID parameters ($k_c = 0.24, \quad T_I = 200.0, \quad T_D = 30.0$).

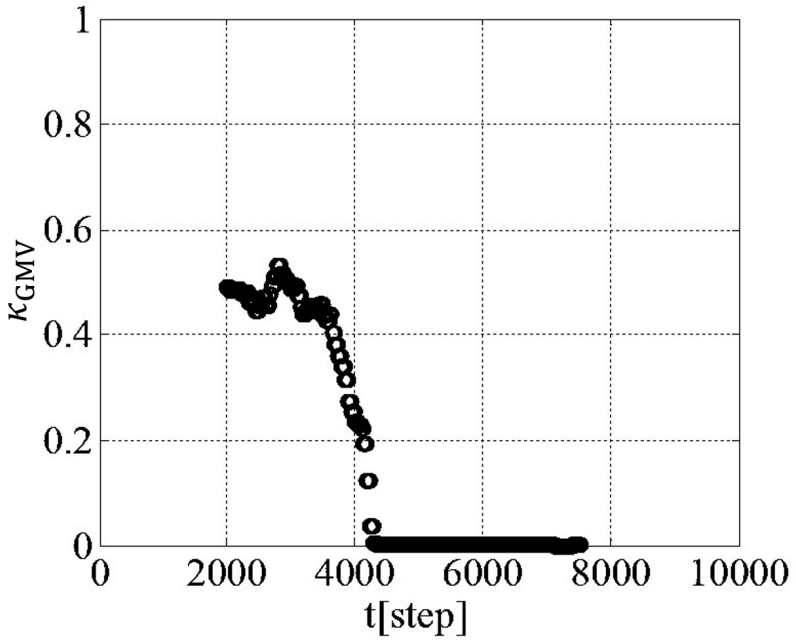


Figure 3.20: Trajectory of $\kappa_{\mathrm{GMV}}$ corresponding to fig. 3.19.

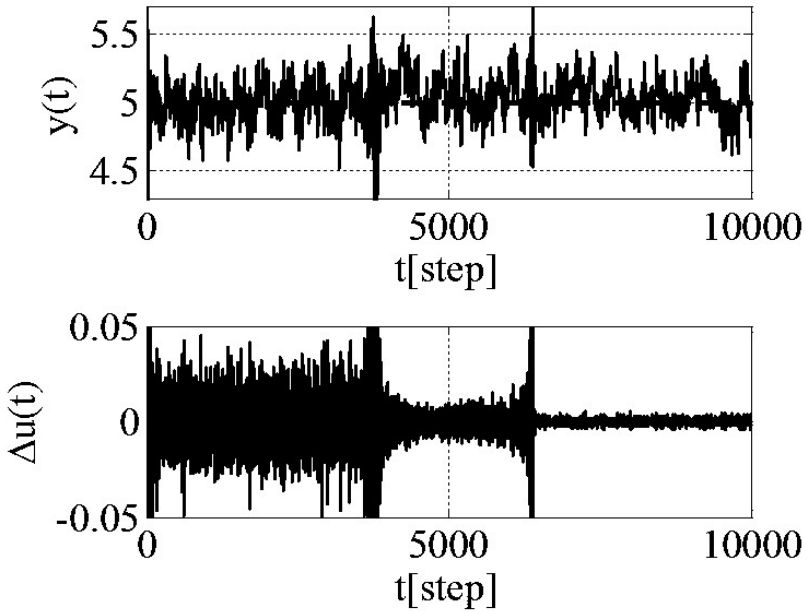


Figure 3.21: Control result obtained using the proposed smart-GMVIndex control scheme.

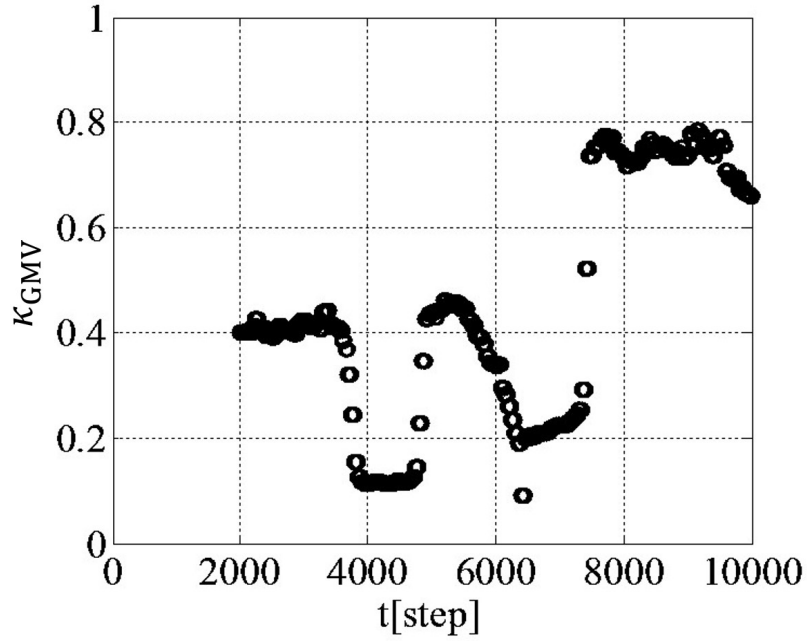


Figure 3.22: Trajectory of $\kappa_{\mathrm{GMV}}$ corresponding to Figure. 3.21.

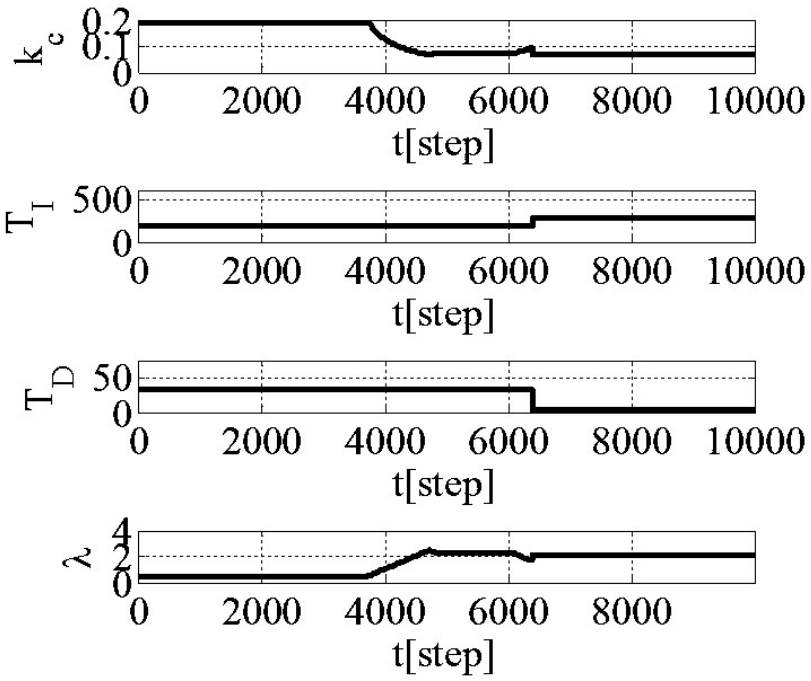


Figure 3.23: Trajectories of PID parameters and $\lambda$ corresponding to Figure. 3.21.

3.23. However, all the PID gains are tuned at approximately the 6500[step] in Figure 3.23. Finally, a variance of $e(t)$ is obtained as 0.023, as shown in Figure 3.21, and a desired variance of $e(t)$ (0.03) is satisfied.

## 3.5 Conclusion

In this chapter, the design of a PD-MVIndex controller and a Smart-GMVIndex controller have been proposed. PID parameters are calculated so that control performance is adaptively improved using a FRIT method. The main feature of the proposed Smart-GMVIndex control scheme was to improve the control performance by adjusting $\lambda$ (1-parameter tuning) when

the control performance is poor. The effectiveness of the proposed scheme was is illustrated by an application to a numerical example.

## Appendix 3.A Deriving Eq. (3.11)

The following equation is obtained from Eqs. (3.1) and (3.3).

$$\begin{aligned}\Delta A(z^{-1})y(t) &= z^{-(k+1)}B(z^{-1})\Delta u(t) + \xi(t) \\ &= z^{-(k+1)}B(z^{-1})C(z^{-1})(r(t) - y(t)) + \xi(t) \end{aligned} \tag{3.65}$$

Now, using $T$ of Eq. (3.12) provides:

$$y(t) = \frac{z^{-(k+1)}B(z^{-1})C(z^{-1})}{T(z^{-1})}r(t) + \frac{1}{T(z^{-1})}\xi(t) \tag{3.66}$$

Substituting Eq. (3.66) into Eq. (3.6) and expanding it provides:

$$\begin{aligned}\phi(t+k+1) &= \frac{B(z^{-1})C(z^{-1})P(z^{-1})}{T(z^{-1})}r(t) \\ &\quad + \frac{P(z^{-1})}{T(z^{-1})}\xi(t+k+1) - P(1)r(t) \\ &= \frac{B(z^{-1})C(z^{-1})(P(z^{-1}) - z^{-(k+1)}P(1) + \Delta A(z^{-1}))}{T(z^{-1})}r(t) \\ &\quad + \frac{P(z^{-1})}{T(z^{-1})}\xi(t+k+1). \end{aligned} \tag{3.67}$$

Let the reference signal be constant ($r(t) = r(t-1) = \cdots = r(t-k-1)$) during the dead time. The first term on the right side of Eq. (3.67) becomes zero, thereby giving the following equation (Eq. (3.10)).

$$\phi(t+k+1) = \frac{P(z^{-1})}{T(z^{-1})}\xi(t+k+1). \tag{3.68}$$

In addition, Eqs. (3.7) and (3.12) make:

$$\begin{aligned} E(z^{-1})T(z^{-1}) &= \Delta A(z^{-1})E(z^{-1}) + z^{-(k+1)}B(z^{-1})C(z^{-1})E(z^{-1}) \\ &= (P(z^{-1}) - z^{-(k+1)}F(z^{-1})) \\ &\quad + z^{-(k+1)}B(z^{-1})C(z^{-1})E(z^{-1}). \end{aligned} \tag{3.69}$$

Multiplying both sides of Eq. (3.10) using the $E(z^{-1})T(z^{-1})$ provides:

$$E(z^{-1})T(z^{-1})\phi(t+k+1) = E(z^{-1})P(z^{-1})\xi(t+k+1). \tag{3.70}$$

In the end, substituting Eq. (3.69) into Eq. (3.70) and using Eqs. (3.10) and (3.13) provide the following equations:

$$\begin{aligned} \phi(t+k+1) &= E(z^{-1})\xi(t+k+1) \\ &\quad + \frac{F(z^{-1}) - B(z^{-1})C(z^{-1})E(z^{-1})}{T(z^{-1})}\xi(t) \qquad (3.71) \\ &= E(z^{-1})\xi(t+k+1) + S(z^{-1})\xi(t). \qquad (3.72) \end{aligned}$$

## Appendix 3.B Deriving Eq. (3.20)

The following equation is obtained from Eqs. (3.68) and (3.72).

$$\phi(t+k+1) = E(z^{-1})\xi(t+k+1) + \frac{T(z^{-1})S(z^{-1})}{P(z^{-1})}\phi(t) \tag{3.73}$$

Multiplying both sides of Eq. (3.73) using the $z^{-(k+1)}$ provides:

$$\phi(t) = \epsilon(t) + \frac{T(z^{-1})S(z^{-1})}{P(z^{-1})}\phi(t-k-1) \tag{3.74}$$

$$\epsilon(t) := E(z^{-1})\xi(t). \tag{3.75}$$

Using a similar approach, $\phi(t)$ is first expressed by the auto-regressive model as follows:

$$\phi(t) = \epsilon(t) + \sum_{i=0}^{M} \alpha_i \phi(t-k-i). \tag{3.76}$$

# Chapter 4

# Application to a Temperature Control System

## 4.1 Introduction

In this chapter, the effectiveness of the proposed schemes (Smart-GMV and PD-MVIndex) is demonstrated through experiments. The equipment consists of a temperature control system in Hiroshima University as shown in Figure 4.1. Figure 4.2 shows the temperature process outline. The system output and control input are the water temperature and the valve aperture of hot water, respectively. The system characteristic can be changed by increasing/decreasing the flow of cold water.

Figure 4.2 shows the measurement of the water temperature $y(t)$ [$^o$C] by using thermometer PT. Its water temperature signal is then sent to a computer. The computer receives the signal by performing A/D conversion. Subsequently, the computer sends the D/A-converted electrical signal to a valve after algorithm processing. The computer then adjusts the valve aperture $u_1(t)$ [%] of the hot water; this is an operational amount, such that the amount of hot water flowing into the tank is adjusted. The operational

Figure 4.1: A temperature process control system.

amount of this experiment has an input limit of $0 \leq u_1(t) \leq 100$.

The aperture $u_2(t)$ of the electrical valve of the cold water is utilized for system change. The hot water in this unit is at a constant temperature, but is stored in another tank without a mixer. This set up may cause the continuous use of warm water to drop or raise the temperature.

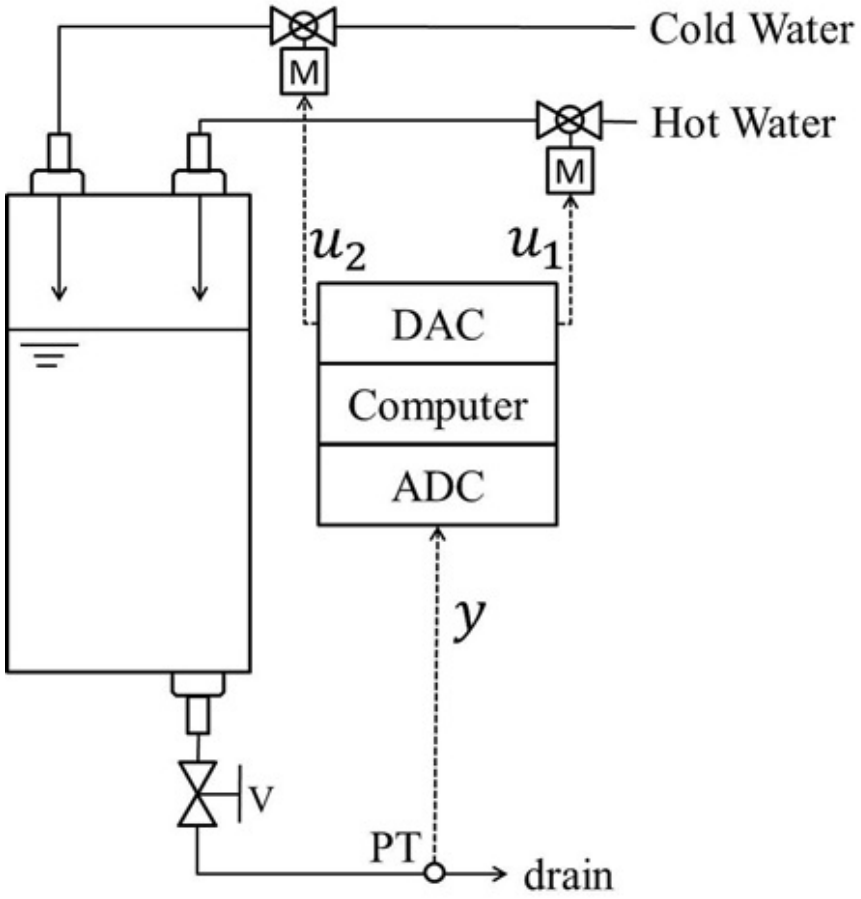


Figure 4.2: Outline illustration of the temperature process control system.

## 4.2 Application and consideration of smart adaptive controllers

### 4.2.1 Application of Smart-GMV controller

In this section, the effectiveness of the proposed Smart-GMV control scheme is demonstrated using a temperature process control system. The sampling time is set as $T_s = 5.0$[s]. In addition, the cold water valve aperture

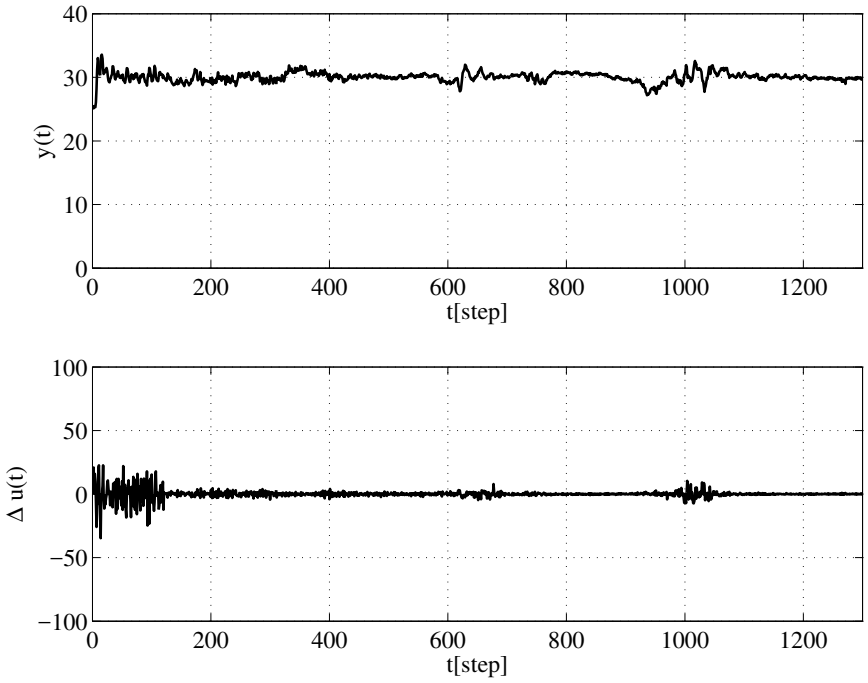


Figure 4.3: Control result obtained using the proposed smart-GMV control scheme in which $\sigma_e^2 = 0.5$.

is changed as follows:

$$u_2(t) = \begin{cases} 50 \ (0 < t \leq 300) \\ 50 - \dfrac{30(t-300)}{700} \ (300 < t \leq 1000) \\ 20 \ (1000 < t \leq 1300) \end{cases} . \tag{4.1}$$

Here, $r(t) = 10$, $m = 3$, $N = 500$, $\lambda_d = 0.03$, and $\Delta\lambda = 0.02$ in chapter 2.2 were set, and $P(z^{-1})$ was designed as follows:

$$P(z^{-1}) = 1 - 1.0268z^{-1} + 0.2636z^{-2}. \tag{4.2}$$

Furthermore, $\sigma_e^2 = 0.5$ was set as the desired variance of control error.

Figures 4.3 and 4.4 show the control result and the trajectories of PID parameters, respectively. In Figures 4.3 and 4.4, the initial PID parameters

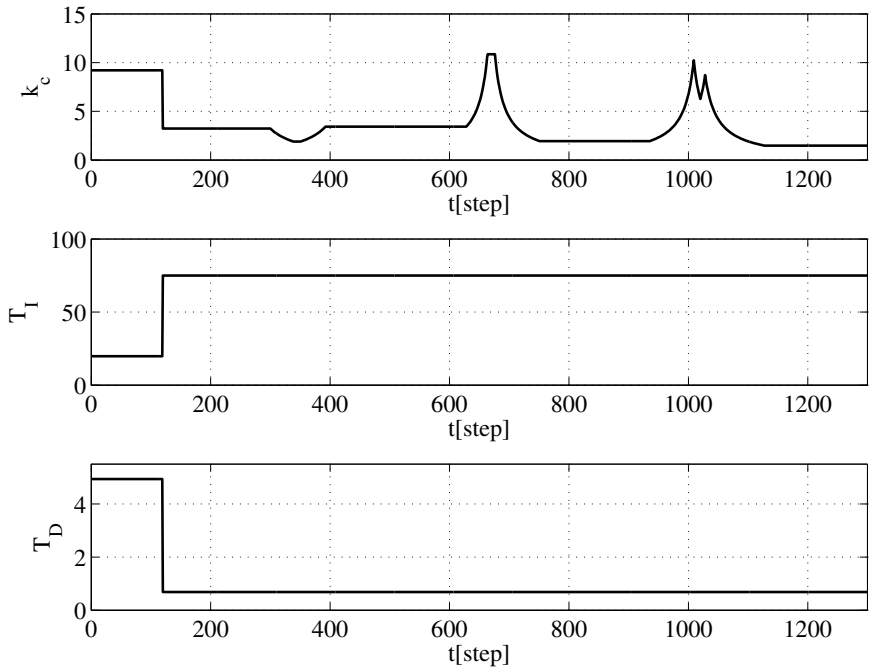


Figure 4.4: Trajectories of PID parameters corresponding to Figure 4.3.

in the first 100[step] are set as follows to obtain closed-loop data:

$$k_c = 9.21, T_I = 19.75, T_D = 4.94, \tag{4.3}$$

which is calculated by the ZN method. The proposed Smart-GMV control scheme (only "1-parameter tuning") is performed at $t = 100$[step]. After 100[step], the variance of control error is 0.41 and the desired control performance ($\sigma_e^2 = 0.5$) is satisfied.

Next, Figures 4.5 and 4.6 show the trajectories of $\lambda$ and variances, respectively. Only $\lambda$ is adjusted in this experiment indicating that only $k_c$ is adjusted because of Eq. (2.19). In Figure 4.5, $\lambda$ is adjusted around the 300, 650, and 950[step] because $\mathcal{E}[\Delta e(t)^2]$ and $\mathcal{E}[\Delta u(t)^2]$ increase considerably than $\mathcal{E}[\Delta e(t)^2]_{\min}$ and $\mathcal{E}[\Delta u(t)^2]_{\min}$ respectively in Figure 4.6. In Figure 4.3,

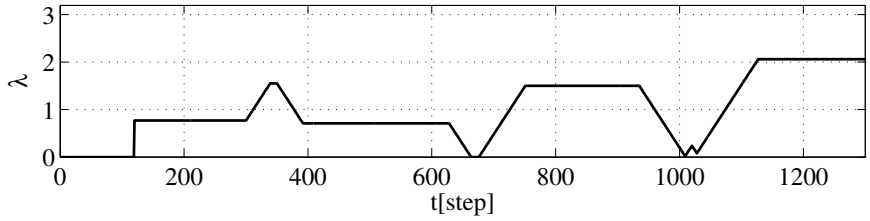


Figure 4.5: Trajectories of $\lambda$ corresponding to Figure 4.3.

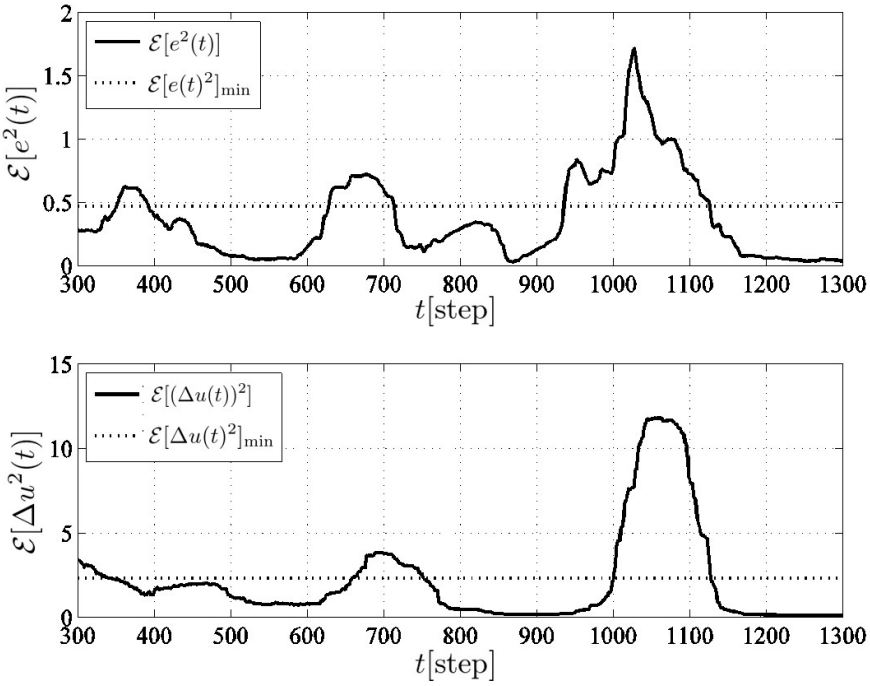


Figure 4.6: Trajectories of the control performance corresponding to Figure 4.3.

temperature at around 650 and 950[step].

Finally, Figure 4.7 shows the control result obtained using only ZN method for comparison. The variance of control error was 1.30, which did not achieve the desired control performance ($\sigma_e^2 = 0.5$). These results verify the effectiveness of 1-parameter tuning.

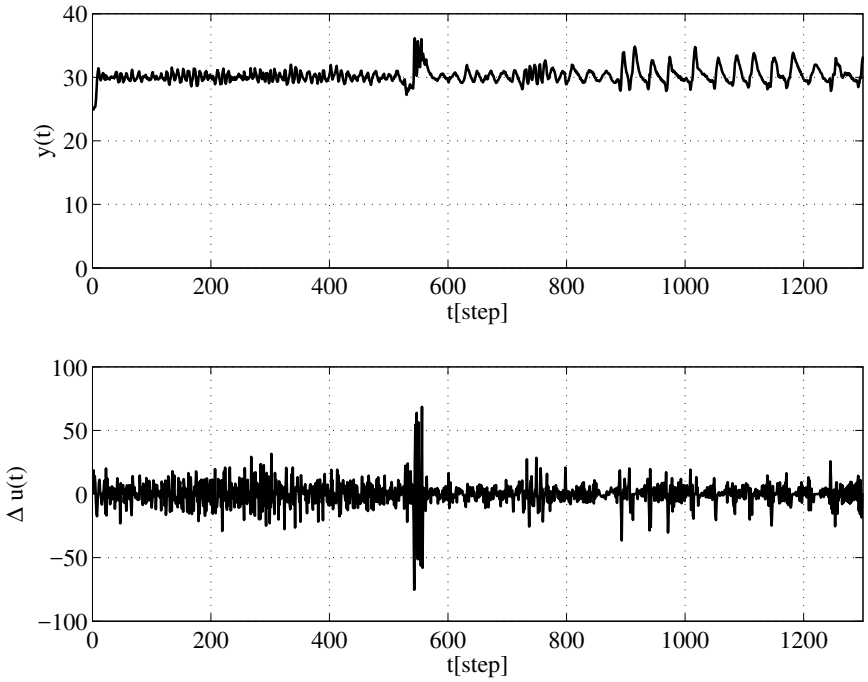


Figure 4.7: Control result obtained using the fixed PID parameters tuned by the ZN method.

### 4.2.2 Application of PD-MVIndex controller

Table 4.1 shows the user-specified parameters used in the an experiment. The sampling time in this experiment was $T_s = 5.0$ [s].

The following PID gains calculated using the ZN method [46] were applied to obtain the closed-loop data:

$$K_P = 10.2, \quad K_I = 1.38, \quad K_D = 9.13 \tag{4.4}$$

A control of up to 300 [step] was performed using the above mentioned PID parameters. The proposed scheme was then applied to the time of 301 [step] by using the input and output data from 150 [step] to 300 [step]. Figure 4.8 shows the control result. Figure 4.9 illustrates the trajectory of the control

Table 4.1: User-specified parameters in an experiment.

| | |
|---|---|
| $r$: target value | 35 |
| $\sigma$: coefficient regarding the rise characteristic | 20 |
| $\delta$: coefficient regarding the decay characteristic | 0 |
| $N$: number of data | 150 |
| $M$: auto-regressive parameter order | 20 |

performance assessment index $\kappa$. The proposed scheme provided the PID gains of Eq. (4.5), where the difference between $\kappa_0$ and $\widetilde{\kappa}_m$ calculated using "fminsearch.m" was $8.63 \times 10^{-7}$.

$$K_P = 5.72, \quad K_I = 0.19, \quad K_D = 0.05 \tag{4.5}$$

Figure 4.10 shows the trajectories of the PID gains corresponding to Figure 4.8. The result of Figure 4.8 indicates that the variance of the input and the output is suppressed after the PID gain adjustment, thereby verifying the effectiveness of the proposed scheme. Figure 4.9 indicates that the control performance $\kappa$ is improved from approximately 0.3 to 0.7. This result verifies the effectiveness of the proposed scheme in the experiment.

Figure 4.11 shows the control result in which $u_2(t)$ is changed from 40[%] to 30[%] during $150 \leq t \leq 450$ as system change. The threshold according to which the control performance deterioration is evaluated is set as 0.4 in advance. The control performance index $\kappa$ is improved when $\kappa$ is below 0.4 after 300[step] in Figure 4.12. Moreover, Figure 4.13 shows the trajectories of PID parameters in which controller parameters are tuned when $\kappa$ is deteriorated effectively.

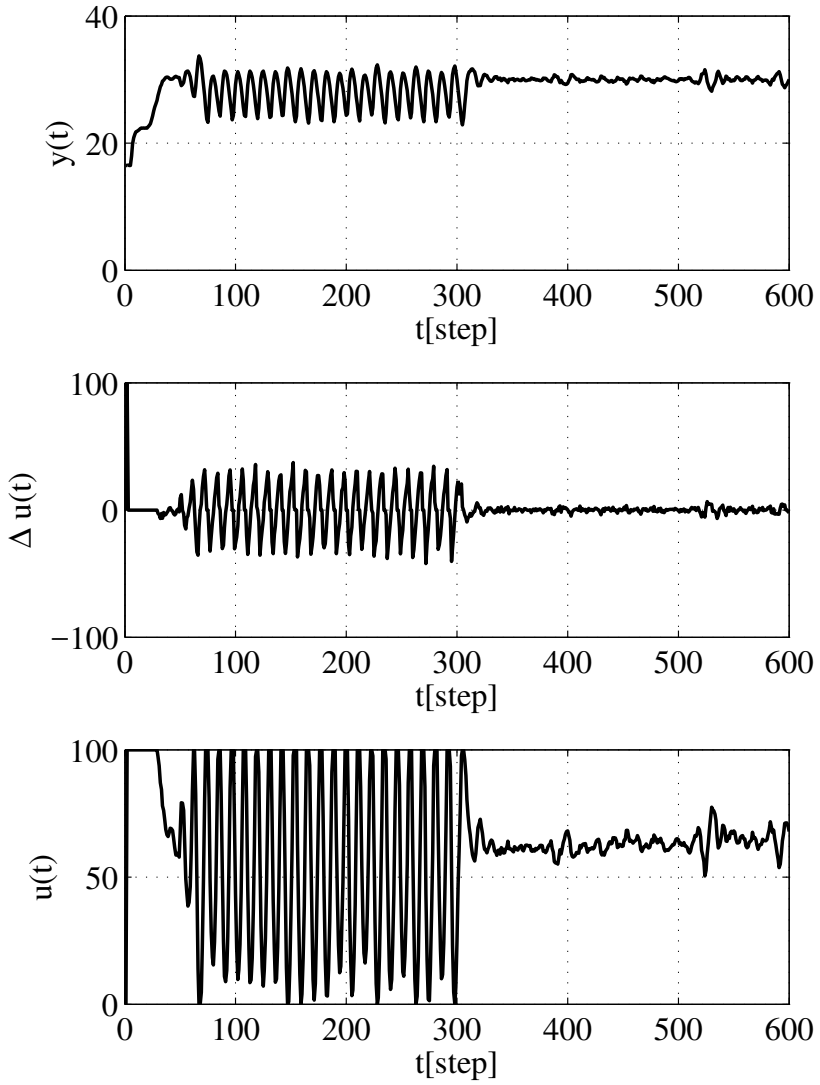


Figure 4.8: Control result obtained using the proposed PD-MVIndex control scheme.

### 4.2.3 Comparing the proposed schemes

Sections 4.2.1 and 4.2.2 describe the control results of the Smart-GMV and PD-MV control schemes. If the controlled object's characteristics, such

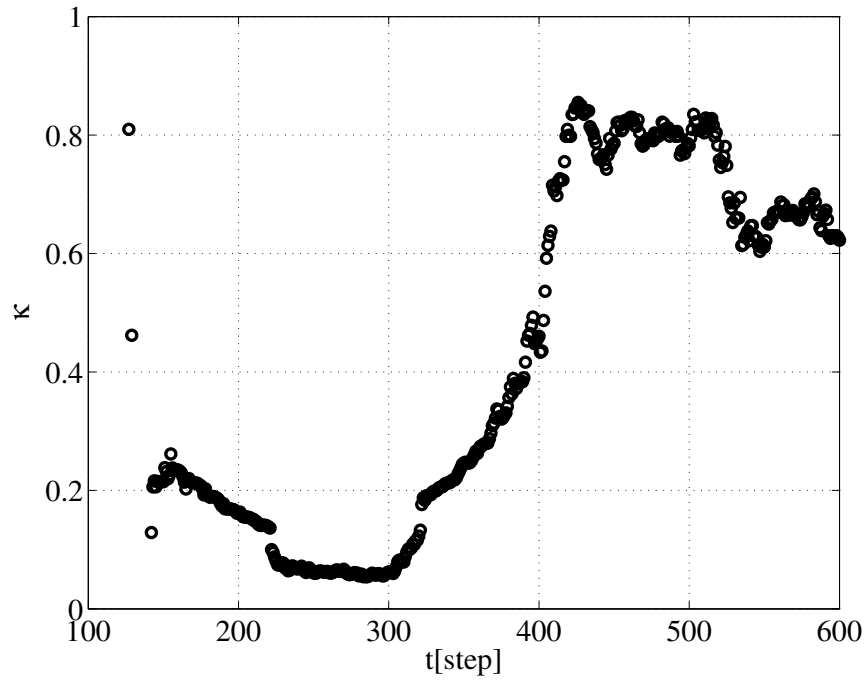


Figure 4.9: Trajectory of $\kappa$ corresponding to Figure 4.8.

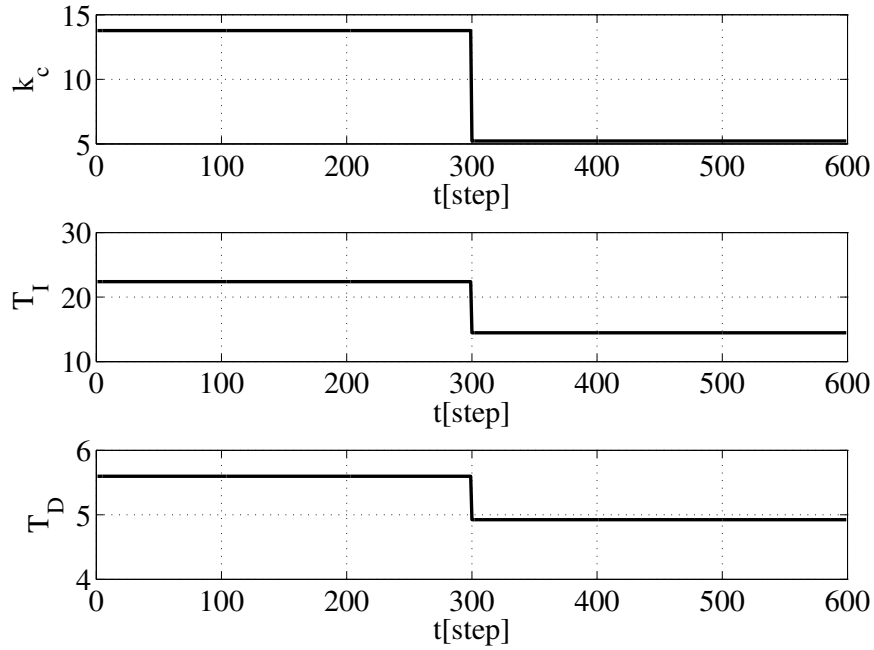


Figure 4.10: Trajectories of the PID parameters corresponding to Figure 4.8.

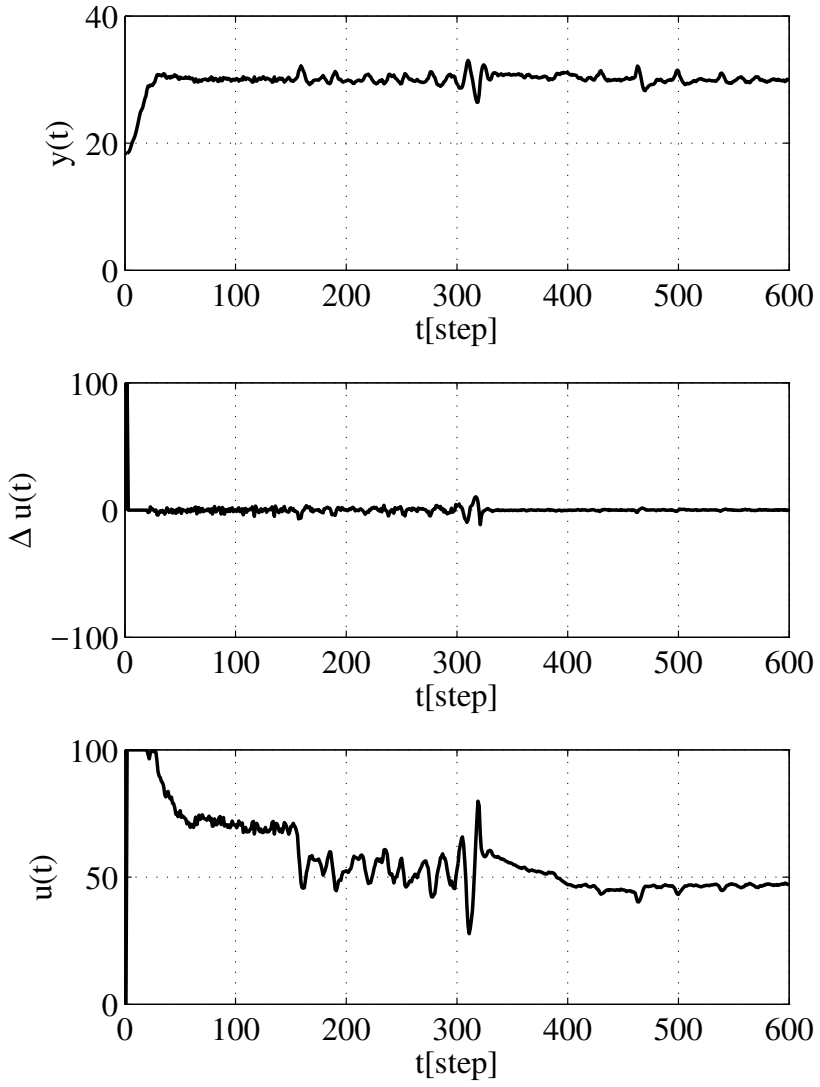


Figure 4.11: Control result by the proposed PD-MVIndex control scheme in system change.

as achievable variance, are well known, the Smart-GMV control scheme outperforms the PD-MV control scheme because the least squared method is utilized for calculating controller parameters and its calculation cost is low.

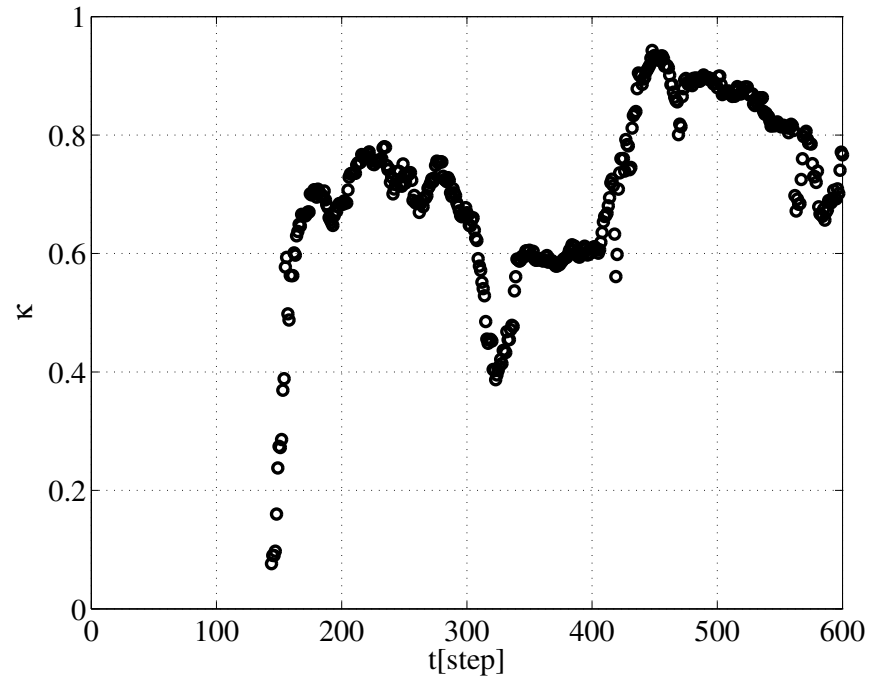


Figure 4.12: Trajectory of $\kappa$ corresponding to Figure 4.11.

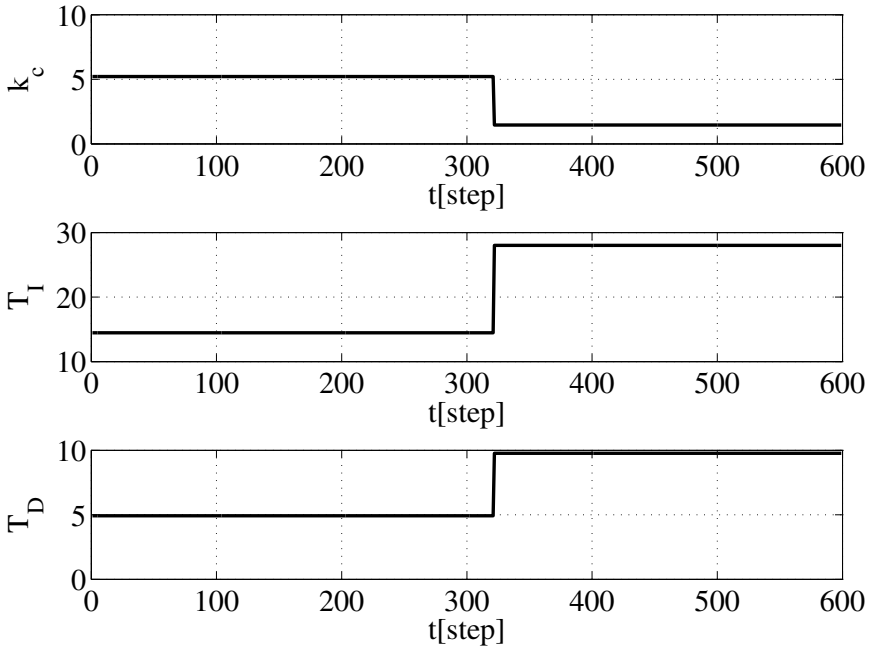


Figure 4.13: Trajectories of the PID parameters corresponding to Figure 4.11.

However, it is difficult to set the threshold $\lambda_d$ in the Smart-GMV because $\lambda_d$ is set based on the achievable control error variance which is changed by the system change. In contrast, in the PD-MVIndex control scheme, it is easy to set the threshold $\alpha$ used to evaluate the control performance deterioration because MV-Index is the normalized performance assessment. However, it is impossible to achieve the desired control performance such as the variance of control error. Therefore, a Smart-GMVIndex control scheme is needed in which the desired control performance can be satisfied, and the setting of the threshold is easy. In this study, the application of the Smart-GMVIndex control to the experiment is not discussed. Therefore, in the near future, it will be applied to the currently used equipment and compared with other proposed schemes.

## 4.3 Conclusion

In this chapter, the effectivenesses of the proposed schemes (Smart-GMV and PD-MVIndex) have been verified using an experimental temperature control system. The system output and control input are water temperature and valve open ratio of hot water, respectively. The equipment can change the system characteristic by increasing/decreasing the flow of cold water. In a Smart-GMV control scheme, it is difficult to set the user-specified parameters, such as threshold, which judges the control performance deterioration. In contrast, in the PD-MVIndex control scheme, it is easy to set the threshold because MV-Index is a normalized performance assessment. In the near future, the proposed Smart-GMVIndex control scheme will be applied to

the currently used equipment and compared with other proposed schemes.

# Chapter 5

# Conclusions

This thesis has presented the smart adaptive control systems in which the controlled object is a process systems. In the proposed scheme, the desired control performance is maintained even if the system characteristic is changed. The control performance in steady state is more important than in the transient state because of the high quality production and/or energy saving. Therefore, the control performance in the steady state has been focused upon, and the controller design methods based on MVC and GMVC have been proposed in this thesis. Moreover, PID gains are tuned through "1-parameter tuning" when the deterioration of control performance is small; however, when the deterioration is large, all controller parameters are adjusted through "controller redesign". In other words, the controller parameters are adjusted by switching the "1-parameter tuning" and "controller redesign" in a smart manner based on control performance. The features of the proposed scheme are as follows:

i) Controller parameters are calculated using a closed-loop data directly.

ii) "Control performance assessment" and "control system design" are integrated.

iii) "1-parameter tuning" and "controller redesign" are switched appropriately, depending on the deterioration of control performance.

Chapter 2 disscussed the proposed Smart-GMV control scheme. First, a scheme is explained according to which the controller parameters are calculated directly without system identification. Next, "1-parameter tuning" and "controller redesign" are switched using the trade-off curve. The trade-off curve shows the relationship between variance of control error and input. Hence, the derivation of the trade-off curve is described along with the algorithm of achieving the desired control performance by using a smart adaptive control law based on GMVC. The effectiveness of this scheme is verified by satisfying the desired control performance for a time-variant system in a numerical example.

In Chapter 3, a smart adaptive control scheme based on FRIT was discussed. An archival desired control performance (variance of control error and input) is different in each controlled objects, and the threshold is difficult to set for switching "1-parameter tuning" and "all controller parameters design". Therefore, in Chapter 3, the control performance assessment (MV-Index and GMV-Index) is focused upon and the controller parameters are calculated such that the control performance assessment is improved using FRIT. The effectiveness of this scheme is confirmed through a numerical example.

In Chapter 4, each smart adaptive control scheme given in Chapters

2 and 3 is applied to the temperature control system. In the temperature control system, the control output and input are the water temperature and the open/close ratio of hot water valve, respectively. Moreover, the system characteristic is changed by increasing/decreasing the flow rate of cold water. Furthermore, the control results of each smart adaptive control scheme are compared.

Finally, the future of smart adaptive control scheme is discussed. Its features include the calculation of controller parameters without system identification to improve the control performance index. Thus, the proposed scheme is effective in not only process industries but also other fields. In particular, it is difficult to obtain a human model in the systems including in the field of cars, constructions, and welfare devices. In these fields, the important aspect is the Kansei because the device evaluations are based on the riding comfort, usability, etc. Althoug the gross domestic product (GDP) in Japan is high, the Japanese happiness level is low, which is reported in a Cabinet Office report [65]. Hence, there is a large gap between "products wealth" of GDP and "mind wealth" of happiness level; this continuously increases every year [66]. Therefore, high quality products such as cars, excavators, and walking support equipment should be designed and controlled to improve the happiness level considering Kansei. For instance, controller parameters of walking support equipment are adaptively adjusted using comfortable information of Kansei. The visualization method of Kansei was proposed recently [67]. Therefore, a smart adaptive Kansei feedback control scheme is required in which Kansei information is fed back into the controller. Here, the Kansei performance index

is defined and controller parameters are tuned to improve the index without system identification. However, the proposed scheme in this thesis did not consider a nonlinear system. For example, a human being is considered as nonlinear and time-variant system. Thus, a data-driven control scheme for nonlinear system should be combined with a smart adaptive controller. In the data-driven control scheme, the database is utilized for stacking data and learning controller parameters. Furthermore, in recent years, the information society has been developing strongly and the information of many devices is sensed. In addition, Internet of Things (IoT) has attracted attention in recent years because of the use of big data is utilized. However, the fusion of IoT and controller is still under development. Therefore, future research must focus on the fusion of IoT and controller, and a smart adaptive control system considering Kansei.

# Bibliography


[1] J. Y. H. P. Whitaker and A. Kezer, ***Design of Model Reference Adaptive Control Systems for Aircraft***. MIT Press, 1958.

[2] E. Mishkin and L. Braun, ***Adaptive Control Systems***. McGraw-Hill, 1961.

[3] K.J.Åström and B. Wittenmark, ***Adaptive Control***. Dover Publications, 2008.

[4] T. Suzuki, ***Adaptive Control (in Japanese)***. Corona, 2001.

[5] I. M. Z. Iwai and H. Ohtsuka, ***Simple Adaptive Control Method: SAC (in Japanese)***. Morikita, 2008.

[6] R. E. Kalman, "Design of a self-optimizing control system," ***ASME***, vol. 80, pp. 468–478, 1958.

[7] L. L. K.J.Åström, U. Borisson and B. Wittenmark, "Theory and applications of self-tuning regulators," ***Automatica***, vol. 13, pp. 457–476, 1977.

[8] D.W.Clarke and P.J.Gawthrop, "Self-tuning control," ***IEE Proc. Control Theory and Aplications***, vol. 126, no. 6, pp. 633–640, 1979.

[9] P.E.Wellstead and M.B.Zarrop, ***Self-Tuning Systems : Control and Signal Processing***. John Wiley & Sons, 1991.

[10] T. Yamamoto and S. Shah, "Design and experimental evaluation of a multivariable self-tuning PID controller," ***Control Theory and Applications***, vol. 151, no. 5, pp. 645–652, 2004.

[11] T.Yamamoto and S.L.Shah, "Design and experimental evaluation of a multivariable self-tuning PID controller," ***IEE Proc. of Control Theory and Applications***, vol. 151, no. 5, pp. 645–652, 2004.

[12] Y. O. T.Yamamoto and S.L.Shah, "Design of a performance-adaptive proportional-integral-derivative controller for stochastic systems," ***Institute of Mechanical Engineering, Part-I, Journal of Systems and Control Engineering***, vol. 222, no. 5, pp. 691–699, 2008.

[13] T.Yamamoto and S.L.Shah, "Design of a performance-adaptive PID controller," ***Proc. of the IEEE International Conference on Networking, Sensing and Control***, pp. 547–552, 2007.

[14] K.Takao, Y.Ohnishi, T.Yamamoto, and T.Hinamoto, "Design of a performance adaptive PID controller based on control performance assessment(in japanese)," ***Trans. Society of Instrument and Control Engineers***, vol. 43, no. 2, pp. 110–117, 2007.

[15] T.Yamamoto, "Design of performance-adaptive PID control system based on modelimg performance assessment(in japanese)," ***IEEJ Transactions on Electronics, Information and Systems***, vol. 27, no. 12, pp. 2101–2108, 2007.

[16] K.Fujii and T.Yamamoto, "One-parameter tuning PID control of a distillation process," ***Proc. International Symposium on Advanced Control of Industrial Processes***, pp. 222–225, 2008.

[17] T.Yamamoto, K.Kawada, H.Kugemoto, and Y.Kutsuwa, "Design and industrial applications of a control performance assessment based PID controller," ***Proc. 15th IFAC Symposium on System Identification***, pp. 729–734, 2009.

[18] T.Yamamoto and S.Wakitani, "Design of a performance-driven self-tuning controller via one-parameter tuning," ***Proc. European Control Conference 2009***, pp. 4019–4024, 2009.

[19] M.Tokuda and T.Yamamoto, "A self-tuning PID controller based on control performance evaluations," ***International Journal of Innovative Computing, Information and Control***, vol. 6, no. 8, pp. 3751–3762, 2010.

[20] L. Ljung, ***System Identification: Theory for the user***. Prentice Hall, 1999.

[21] S.Adachi and A.Sano, "System indentification : From fundamentals to recent topics[2] (in japanese)," ***Journal of the Japan Society For Simulation Technology***, vol. 12, no. 2, pp. 128–135, 1993.

[22] H.Hjalmarsson, S.Gunnarson, and M.Gevers, "A convergent iterative restricted complexity control design scheme," ***Proc. of the 33rd IEEE conference on decision and control***, vol. 2, pp. 1735–1740, 1994.

[23] H.Hjalmarsson, M.Gevers, S.Gunnarsson, and O.Lequin, "Iterative feedback tuning : theory and applications," ***IEEE Control System Magazine***, vol. 18, no. 4, pp. 26–41, 1998.

[24] H.Hjalmarsson, "Iterative feedback tuning –an overview," ***Int. J. Adapt. Control Signal Processing***, vol. 16, no. 5, pp. 373–395, 2002.

[25] K.Hamamoto, T.Fukuda, and T.Sugie, "Iterative feedback tuning of controllers for a two-mass-spring system," ***Control Engineering Practice***, vol. 11, pp. 1061–1068, 2003.

[26] M.Nakamoto, "Direct PID parameter tuning method using experimental data (¡special issue¿parameters tuning in PID control) (in japanese)," ***Trans. of the Institute of Systems, Control and Information Engineers***, vol. 50, no. 12, pp. 447–452, 2006.

[27] M.C.Campi, "Virtual reference feedback tuning (VRFT) : A direct method for the design of feedback controllers," ***Automatica***, vol. 38, no. 8, pp. 1337–1346, 2002.

[28] A.Lecchini, M.C.Campi, and S.M.Savaresi, "Virtual reference feedback tuning for two degree of freedom controllers," ***International Journal of Adaptive Control and Signal Processing***, vol. 16, no. 5, pp. 355–371, 2002.

[29] M.C.Campi, A.Lecchini, and S.M.Savaresi, "An application of the virtual reference feedback tuning (VRFT) method to a benchmark active suspension system," ***European Journal of Control***, vol. 9, pp. 66–76, 2003.

[30] F.Previdi, T.Schauer, S.M.Savaresi, and K.J.Hunt, "Data-driven control design for neuroprotheses : A virtual reference feedback tuning (VRFT) approach," ***IEEE Trans. on Control Systems Technology***, vol. 12, no. 1, pp. 176–182, 2004.

[31] M.C.Campi, "Direct, nonlinear control design : the virtual reference feedback tuning (VRFT) approach," ***IEEE Trans. Automatic Control***, vol. 51, no. 1, pp. 14–27, 2006.

[32] S.Soma, O.Kaneko, and T.Fujii, "A new approach to parameter tuning of controllers by using one-shot experimental data : A proposal of fictitious reference iterative tuning (in japanese)," ***Trans. of the Institute of Systems, Control and Information Engineers***, vol. 17, no. 12, pp. 528–536, 2004.

[33] O.Kaneko, S.Souma, and T.Fujii, "A fictitious reference iterative tuning (FRIT) in the two-degree of freedom control scheme and its application to closed loop system identification," ***Proc. of 16th IFAC World congress (CD-ROM)***, 2005.

[34] O.Kaneko, K.Yoshida, K.Matsumoto, and T.Fujii, "A new parameter tuning for controllers based on least-squares method by using one-shot closed loop experimental data : An extension of fictitious reference iterative tuning (in japanese)," ***Trans. of the Institute of Systems, Control and Information Engineers***, vol. 18, no. 11, pp. 400–409, 2005.

[35] K.Hosokawa, S.Wakitani, and T.Yamamoto, "Design of a data-driven model-free type GMV-PID control system (in japanese)," ***Trans. of the Institute of Electrical Engineers of Japan. C***, vol. 133, no. 6, pp. 1103–1108, 2013.

[36] S.Masuda, M.Kano, Y.Yasuda, and G.D.Li, "A fictitious reference iterative tuning method with simulations delay parameter tuning of the reference model," ***IJICIC***, vol. 6, no. 7, pp. 2927–2939, 2010.

[37] Y.Ohnishi and T.Yamamoto, "A design of a FRIT based nonlinear PID controller," ***10th IFAC International Workshop on the Adaptation and Learning in Control and Signal Processing***, pp. 152–155, 2010.

[38] Y.Wakasa, S.Kanagawa, T.Kanya, and Y.Nishimura, "FRIT with deadzone compensation and its application to ultrasonic motors," ***10th IFAC International Workshop on the Adaptation and Learning in Control and Signal Processing***, pp. 156–161, 2010.

[39] I.Mizumoto and H.Tanaka, "Model free design of parallel feedforward compensator for adaptive output feedback control via FRIT with t-s fuzzy like model," ***10th IFAC International Workshop on the Adaptation and Learning in Control and Signal Processing***, pp. 139–144, 2010.

[40] S.Masuda, "PID controller tuning based on disturbance attenuation FRIT using one-shot experimental data due to a load change disturbance," ***Proc. of 2nd IFAC Conference on Advances in PID Control***, pp. 92–97, 2012.

[41] T.Shigemasa, Y.Negishi, and Y.Baba, "From FRIT of a pd feedback loop to process modelling and control system design," ***Proc. of 11th IFAC International Workshop on Adaptation and Learning in Control and Signal Processing***, pp. 337–342, 2013.

[42] F.Uozumi, O.Kaneko, and S.Yamamoto, "Fictitious reference iterative tuning of disturbance observers for attenuation of the effect of periodic unknown exogenous signals," ***Proc. of 11th IFAC International Workshop on Adaptation and Learning in Control and Signal Processing***, pp. 576–581, 2013.

[43] T. J. Harris, "Assessment of closed loop performance," ***Canadian J. Chemical Engineering***, vol. 67, pp. 856–861, 1989.

[44] B. Huang and S. L. Shah, ***Performance Assessment of Control Loops: Theory and Applications***. Springer-Verlag, 1999.

[45] B.Huang, "A pragmatic approach towards assessment of control loop performance," ***International Journal of Adaptive Control and Signal Processing***, vol. 17, pp. 589–608, 2003.

[46] J.G.Ziegler and N.B.Nichols, "Optimum settings for automatic controllers," ***Trans. ASME***, vol. 64, no. 8, pp. 759–768, 1942.

[47] K.L.Chien, J.A.Hrones, and J.B.Reswick, "On the automatic control of generalized passice systems," ***Trans. ASME***, vol. 74, pp. 175–185, 1952.

[48] N.Suda and etal, ***PID Control (in Japanese)***. Asakura Publishing Company, 1992.

[49] R.Vilanova and A.Visioli, ***PID control in the Third Millennium : lessons learned and new approaches***. Springer, 2012.

[50] K.J.Åström and T. Hägglund, "The future of PID control," ***Control Engineering Practice***, vol. 9, no. 11, pp. 1163–1175, 2001.

[51] S. Y. O. Kaneko, Y. Wadagaki and S. Yamamoto, "FRIT for non-minimum phase systems in the 2DOF control architecture: Simultaneous attainment of controllers and models," ***Trans. on SICE***, vol. 7, no. 1, pp. 35–40, 2014.

[52] S. H. S. Wakitani and T. Yamamoto, "Design and application of a direct gmv-based PID controller," ***Proc. of the 2012 International Conference on Advanced Mechatronic System***, pp. 541–546, 2012.

[53] T. Yamamoto, "The role of 'control' in chemical processes, - energy saving by 'control' - (in japanese)," ***Trans. on SICE***, vol. 51, no. 10, pp. 962–967, 2012.

[54] T. J. H. L. Desborough, "Performance assessment measures for univariate feedback control," ***The Canadian Journal of Chemical Engineering***, vol. 70, pp. 1186–1197, 1992.

[55] B.Huang and S.L.Shah, ***Performance Assessment of Control Loops: Theory and Applications***. Springer-Verlag, 1999.

[56] M. Jelali, ***Control Performance Management in Industrial Automation***. Springer-Verlag, 2013.

[57] M. K. (*edit.*), ***Control Performance Monitoring - For Practical Use in Process Industries - (in Japanese)***. Springer-Verlag, 2005.

[58] S. Omatu and T. Y. (*edit.*), ***Self-Tuning Control (in Japanese)***. Corona Publishing Co. Ltd., 1996.

[59] T. Yamamoto and M. Kaneda, "A design of self-tuning PID controllers based on the generalized minimum variance control law (in japanese)," ***Trans. of the Institute of Systems, Control and Information Engineers***, vol. 11, no. 1, pp. 1–9, 1998.

[60] E.Mishkin and L.Braun, ***Adaptive Control Systems***. McGraw-Hill, 1961.

[61] I.D.Landau and M.Tomizuka, ***Theory and Practice of Adaptive Control Systems (in Japanese)***. Ohm Publishing Co. Ltd., 1981.

[62] M. Kanai, ***Introduction to Robust Adaptive Control (in Japanese)***. Ohm Publishing Co. Ltd., 1989.

[63] T. Y.Ohnishi, K.Takao and S.L.Shah, "Design of a PID controller with a performance-driven adaptive mechanism," ***Proc. of American Control Conference***, vol. 70, pp. 1359–1364, 2007.

[64] O. Kaneko, "Data-driven controller tuning: FRIT approach," ***Proc. of 11th IFAC International Workshop on Adaptation and Learning in Control and Signal Processing***, pp. 326–336, 2013.

[65] J. The Commission on Measuring Well-being, ***Measuring National Well-Being – Proposed Well-being Indicators–***. Cabinet Office, Government of Japan, 2011.

[66] W. P. on the National Lifestyle, ***A comfortable way of life for the Japanese people, founded on personal relationships***. Cabinet Office, Government of Japan, 2007.

[67] "Nurturing mental wealth center of kansei innovation," ***URL: http://coikansei.hiroshima-u.ac.jp/***.

# Publication Lists


[1] Takuya Kinoshita, Shin Wakitani, Masayoshi Nakamoto and Toru Yamamoto, "Design of a Data-Oriented Smart Adaptive Controller (in Japanese)", ***Transactions of the Institute of Systems, Control and Information Engineers***, vol. 27, no. 3, pp. 87-94, 2014.

[2] Takuya Kinoshita, Masaru Katayama and Toru Yamamoto, "Performance-Driven PID Control based upon Discrete-Time IMC Tuning (in Japanese)", ***Transaction of the Institute of Electrical Engineers of Japan. C***, vol. 134, no. 9, pp. 1221-1227, 2014.

[3] Takuya Kinoshita, Akinori Inoue, Yoshihiro Ohnishi and Toru Yamamoto, "Design and Experiment Evaluation of a Performance-Driven Control System Using a FRIT (in Japanese)", ***Transactions of the Institute of Systems, Control and Information Engineers***, vol. 29, no. 5, pp. 202-209, 2016.

[4] Takuya Kinoshita and Toru Yamamoto, "Design of a Data-Oriented Cascade Control System (in Japanese)", ***Transaction of the Institute of Electrical Engineers of Japan. C***, vol. 136, no. 5, pp. 703-709, 2016

[5] Akihiro Ishimura, Masayoshi Nakamoto, Takuya Kinoshita and Toru Yamamoto, "An Adjustment of Reference Tracking PID Controllers for a First-order System with a Dead Time (in Japanese)", ***Transaction of the Institute of Electrical Engineers of Japan. C***, vol. 136, no. 5, 2016.

[6] Takuya Kinoshita, Shinichi Imai, Kazushige Koiwai and Toru Yamamoto, "Design of a Data-Oriented Control System for Walking Support", ***Transaction of the Institute of Electrical Engineers of Japan. C***, vol. 136, no. 7, 2016.

[7] Toru Yamamoto, Takuya Kinoshita, Yoshihiro Ohnishi and Sirish L. Shah, "Design and Experimental Evaluation of a Performance-Driven PID controller", ***Transaction of the Journal of Robotics and Mechatron-***

***ics***, vol. 28, no. 5, pp. 616-624, 2016.

[8] Yasuhito Oshima, Takuya Kinoshita, Kazushige Koiwai, Toru Yamamoto, Takao Nanjo, Yoichiro Yamazaki, and Yoshiaki Fujimoto, "Data-Driven Torque Controller for a Hydraulic Excavator", ***Transaction of the Journal of Robotics and Mechatronics***, vol. 28, no. 5, pp. 759-775, 2016.

[9] Ryusei Nakano, Takuya Kinoshita, Shin Wakitani and Toru Yamamoto, "Design of a Performance-Driven Control System Using a Support Vector Machine (in Japanese)", ***Transaction of the Institute of Electrical Engineers of Japan. C***, vol. 137, no. 1, pp. 89-95, 2017.

[10] Tomohiro Hayashida, Toru Yamamoto, Takuya Kinoshita, Ichiro Nishizaki, Shinya Sekizaki and Naoto Hiratsuka, "System change detection method using recurrent neural networks (in Japanese)", ***Transaction of the Institute of Electrical Engineers of Japan. C***, vol. 137, no. 2, 2017 (to appear).

# International Conference Papers

[1] Takuya Kinoshita, Akihiro Kishimoto and Toru Yamamoto, "Design of a Smart Adaptive Control System Based on Control Performance Evaluation", ***Proceedings of the SICE Annual Conference 2014***, pp. 275–280, Sapporo 2014.

[2] Takuya Kinoshita, Masaru Katayama and Toru Yamamoto, "Design of a Performance-Adaptive PID Controller Based on IMC Tuning Scheme", ***Proceedings of the Advanced Control of Industrial Processes 2014***, pp. 351–355, Hiroshima 2014.

[3] Takuya Kinoshita, Shin Wakitani and Toru Yamamoto, "Design and Experimental Evaluation of a Predictive PID Controller", ***Proceedings of 2015 IEEE 20th Conference on Emerging Technologies & Factory Automation***, Luxembourg City 2015.

[4] Takuya Kinoshita and Toru Yamamoto, "Design of a Smart Adaptive Control System", ***Proceedings of the 9th International Symposium on Advanced Control of Chemical Processes***, pp. 1310–1315,Whistler 2015.

[5] Takuya Kinoshita, Yoshihiro Ohnishi and Toru Yamamoto, "A Practical Control Performance Index and PID Controller Design", ***Proceedings of the 10th Asian Control Conference***, Kota Kinabalu 2015.

[6] Yoshihiro Ohnishi, Takuya Kinoshita, Akinori Inoue, Toru Yamamoto and Sirish Shah, "A Design of Data-Driven PID Controller Based on Steady-State Performance", ***Proceedings of the 42nd Annual Conference of IEEE Industrial Electronics Society***, Firenze 2016.

[7] Takuya Kinoshita, Kazushige Koiwai, Toru Yamamoto, Takao Nanjo, Yoichiro Yamazaki and Yoshiaki Fujimoto, "Design of a Data-Driven Control System for a Hydraulic Excavator", ***Proceedings of the 2016 International Conference on Artificial Life and Robotics***, pp.393–396, Naha 2016.

[8] Takuya Kinoshita and Toru Yamamoto, "Design of a Data-Oriented Kansei Feedback System", ***Proceedings of the 2017 International Conference on Artificial Life and Robotics***, pp. 429–432, Miyazaki 2017.